Brain Structure and Function (2019) 224:1219–1244
https://doi.org/10.1007/s00429-019-01831-x

ORIGINAL ARTICLE

Cartography of hevin-expressing cells in the adult brain reveals prominent expression in astrocytes and parvalbumin neurons

Raphaële Mongrédien[1] · Amaia M. Erdozain[2,3] · Sylvie Dumas[4] · Laura Cutando[5] · Amaia Nuñez del Moral[2] · Emma Puighermanal[5] · Sara Rezai Amin[1] · Bruno Giros[1] · Emmanuel Valjent[5] · J. Javier Meana[2,3] · Sophie Gautron[1] · Luis F. Callado[2,3] · Véronique Fabre[1] · Vincent Vialou[1]

Received: 8 February 2018 / Accepted: 8 January 2019 / Published online: 17 January 2019

Abstract

Hevin, also known as SPARC-like 1, is a member of the secreted protein acidic and rich in cysteine family of matricellular proteins, which has been implicated in neuronal migration and synaptogenesis during development. Unlike previously characterized matricellular proteins, hevin remains strongly expressed in the adult brain in both astrocytes and neurons, but its precise pattern of expression is unknown. The present study provides the first systematic description of hevin mRNA distribution in the adult mouse brain. Using isotopic in situ hybridization, we showed that hevin is strongly expressed in the cortex, hippocampus, basal ganglia complex, diverse thalamic nuclei and brainstem motor nuclei. To identify the cellular phenotype of hevin-expressing cells, we used double fluorescent in situ hybridization in mouse and human adult brains. In the mouse, hevin mRNA was found in the majority of astrocytes but also in specific neuronal populations. Hevin was expressed in almost all parvalbumin-positive projection neurons and local interneurons. In addition, hevin mRNA was found in: (1) subsets of other inhibitory GABAergic neuronal subtypes, including calbindin, cholecystokinin, neuropeptide Y, and somatostatin-positive neurons; (2) subsets of glutamatergic neurons, identified by the expression of the vesicular glutamate transporters VGLUT1 and VGLUT2; and (3) the majority of cholinergic neurons from motor nuclei. Hevin mRNA was absent from all monoaminergic neurons and cholinergic neurons of the ascending pathway. A similar cellular profile of expression was observed in human, with expression of hevin in parvalbumin interneurons and astrocytes in the cortex and caudate nucleus as well as in cortical glutamatergic neurons. Furthermore, hevin transcript was enriched in ribosomes of astrocytes and parvalbumin neurons providing a direct evidence of hevin mRNAs translation in these cell types. This study reveals the unique and complex expression profile of the matricellular protein hevin in the adult brain. This distribution is compatible with a role of hevin in astrocytic-mediated adult synaptic plasticity and in the regulation of network activity mediated by parvalbumin-expressing neurons.

Keywords Hevin · Matricellular protein · Parvalbumin neurons · Astrocytes · Glutamatergic neurons · In situ hybridization

Abbreviations

3V	3rd ventricle
4V	4th ventricle
AD	Anterodorsal thalamic nucleus
ac	Anterior commissure
AD	Anterodorsal thalamic nucleus
AM	Anteromedial thalamic nucleus

Raphaële Mongrédien and Amaia M. Erdozain contributed equally to this work.

Electronic supplementary material The online version of this article (https://doi.org/10.1007/s00429-019-01831-x) contains supplementary material, which is available to authorized users.

✉ Vincent Vialou
vincent.vialou@inserm.fr

[1] Sorbonne Université, INSERM, CNRS, Neuroscience Paris Seine, Institut de Biologie Paris Seine, Paris, France

[2] Department of Pharmacology, University of the Basque Country, UPV/EHU, Bizkaia, Spain

[3] Centro de Investigación Biomédica en Red de Salud Mental (CIBERSAM), Madrid, Spain

[4] Oramacell, Paris, France

[5] IGF, CNRS, INSERM, University of Montpellier, Montpellier, France

Amb	Ambiguus nucleus
AON	Anterior olfactory nucleus
APT	Anterior pretectal nucleus
AVL	Anteroventral thalamic nucleus, lateral part
AVM	Anteroventral thalamic nucleus, medial part
Berg.	Bergman glia
BLA	Basolateral amygdala
CA1-3	Cornu ammonis
Cb	Cerebellum
cc	Corpus callosum
ChP	Choroid plexus
Cl	Claustrum
CPu	Caudate putamen
Cx	Cortex
DBB	Diagonal band of Broca
DG	Dentate gyrus
DLG	Dorsal lateral geniculate nucleus
DM	Dorsomedial hypothalamic nucleus
DRc	Dorsal raphe nucleus caudal part
GCL	Granule cell layer
Gl	Glomerular layer
HDB	Nucleus of the horizontal limb of the diagonal band
Hipp	Hippocampus
IC	Inferior colliculus
ic	Internal capsule
IPN	Interpeduncular nucleus
LDDM	Laterodorsal thalamic nucleus, dorsomedial part
LDTg	Laterodorsal tegmental nucleus
LGP	Lateral globus pallidus
LH	Lateral hypothalamic area
LHb	Lateral habenula nucleus
LP	Lateral posterior thalamic nucleus
LS	Lateral septal nucleus
LSd	Lateral septal nucleus, dorsal part
LV	Lateral ventricle
MCPO	Magnocellular preoptic nucleus
MD	Mediodorsal thalamic nucleus
MGP	Medial globus pallidus
Mi	Mitral cell layer of the olfactory bulb
ML	Molecular layer
Mol	Molecular layer of the dentate gyrus
MPO	Medial preoptic nucleus
MRc	Median raphe nucleus caudal part
MS	Medial septum
Mve	Medial vestibular nucleus
Or	Oriens layer of the hippocampus
PAG	Periaqueductal gray
PCL	Purkinje cell layer
Pn	Pontine nucleus
Po	Posterior thalamic nuclear group
PrS	Presubiculum
PVA	Paraventricular thalamic nucleus, anterior part
Rad	Stratum radiatum of the hippocampus
Re	Reuniens thalamic nucleus
RMC	Red nucleus, magnocellular part
RN	Red nucleus
Rt	Reticular thalamic nucleus
SC	Superior colliculus
SNc	Substantia nigra pars compacta
SNr	Substantia nigra pars reticulata
Sp5	Spinal trigeminal nucleus
Tg	Tegmental nucleus
VA	Ventral anterior thalamic nucleus
Vest	Vestibular nucleus
VP	Ventral pallidum
VPM	Ventral posteromedial thalamic nucleus
VTA	Ventral tegmental area
ZI	Zona incerta
III	Oculomotor nucleus
V	Motor trigeminal nucleus
VI	Abducens nucleus
VII	Facial nucleus
VIII	Cochlear nucleus
IX	Glossopharyngeal nucleus
X	Dorsal motor nucleus of vagus
XII	Hypoglossal nucleus

Introduction

Hevin, also known as SPARC-like 1 (SPARCL1), ECM2 or Mast9, belongs to the matricellular proteins of the SPARC (secreted protein acidic and rich in cysteine) family, a class of nonstructural extracellular matrix (ECM) molecules that regulate cell morphology, proliferation and migration (Girard and Springer 1996; Gongidi et al. 2004; Sage and Bornstein 1991; Sullivan et al. 2008). These matricellular proteins include structurally diverse proteins such as thrombospondins 1 and 2, tenascins, SPARC and hevin (Murphy-Ullrich and Sage 2014), which interact with other classes of ECM proteins as well as with cytokines, proteases, neurotrophic factors and cell surface receptors (Bornstein 1995). In the developing central nervous system (CNS), hevin modulates neuronal migration and synaptogenesis. Specifically, hevin helps terminate neuronal migration through its antiadhesive properties (Gongidi et al. 2004). At postnatal day (P) 15, a period of intense synaptogenesis, release of hevin promotes the apposition and stabilization of pre- and post-synaptic specialized junction elements by clustering trans-synaptic adhesion molecules, neurexin, and neuroligin (Risher et al. 2014; Singh et al. 2016). Although hevin is strongly expressed in the adult CNS (Eroglu 2009; Lloyd-Burton and Roskams 2012; Mendis et al. 1996; Mothe and Brown 2002; Weaver et al. 2011), its impact on adult brain function is currently unknown. In animal models of epilepsy,

ischemia and injury, hevin is induced in reactive astrocytes, suggesting that it might participate in neuronal remodeling in pathological conditions in the adult stage (Lively and Brown 2008a, b; Lively et al. 2011; Mendis et al. 2000).

Neuroanatomical studies have identified the cellular phenotype of hevin-expressing cells only during development. From embryonic day (E) 10.5 to P1, hevin is expressed in radial glial cells and vascular endothelial cells and is absent from neuroblasts (Lloyd-Burton and Roskams 2012; McKinnon et al. 2000). After the first postnatal week, in which the vast majority of radial glial cells undergo differentiation into astrocytes, hevin is expressed in astrocytes while progressively disappearing from blood vessels, and is absent from microglia (Lively et al. 2011; Lloyd-Burton and Roskams 2012; Risher et al. 2014). Hevin starts to be expressed in subsets of neurons at P1 and remains expressed in adult neurons (Kucukdereli et al. 2011; Lively and Brown 2008c; Lively et al. 2011; Lloyd-Burton and Roskams 2012; McKinnon et al. 2000; Mendis et al. 1996; Risher et al. 2014). The spatio-temporal expression profile of hevin is strikingly different from other matricellular proteins such as SPARC, its closest homologue, whose expression decreases throughout development and is mostly absent from neurons (Eroglu 2009; Jones et al. 2011; Kucukdereli et al. 2011). However, studies describing the precise distribution of hevin in the entire adult brain are lacking, and the phenotype of the neurons expressing hevin is unknown.

Here, we determined the regional distribution of hevin throughout the adult mouse brain using isotopic in situ hybridization (ISH). For comparison purposes, we also determined the distribution of SPARC mRNA. To determine the cellular phenotype of hevin-expressing cells, we performed double fluorescent in situ hybridization (FISH) with probes targeting hevin and markers of astrocytes, glutamatergic neurons, gamma-aminobutyric acid (GABA) neuron subtypes, monoaminergic and cholinergic neurons. In addition, we characterized the phenotype of hevin mRNA-expressing cells in two human brain regions, the prefrontal cortex and the caudate nucleus.

Materials and methods

Animals

All experiments were performed in conformity with the European Union laws and policies for the use of animals in neuroscience research (European Committee Council Directive 2010/63/EU), and were approved by the local animal research committee. Nine- and twelve-week-old male and female C57BL6J mice were housed in groups under standard conditions at 22 ± 1 °C and a 12 h light/dark cycle, with food and water provided ad libitum.

Preparation of mouse brain sections

Brains were quickly removed after decapitation and frozen at − 30 °C in 2-methylbutane. Coronal frozen sections (16 µm) were prepared with a cryostat at − 20 °C, thaw-mounted onto poly-L-lysine-coated glass slides (Superfrost Plus, Menzel Glaser, Braunschweig, Germany) and stored at − 80 °C until usage. The entire brain was cut and sections were serially mounted with a step of 144 µm between two consecutive sections.

Human brain samples

Human brain samples from 12 subjects who died from sudden and violent causes were obtained at autopsy in the Basque Institute of Legal Medicine in Bilbao, Spain. All subjects were free of psychiatric or neurological disorders based on medical history, postmortem tissue examinations and a toxicological screening on blood at autopsy (detection of antidepressants, antipsychotics, other psychotropic drugs, and ethanol). Samples from the prefrontal cortex and caudate nucleus ($n = 8$) were dissected at the time of autopsy and immediately stored at − 70 °C until assayed. These two specific areas were chosen, as they are representative of the diversity of hevin-expressing cell types in the mouse brain, i.e., astrocytes, parvalbumin neurons, and glutamatergic neurons. The demographic and brain sample characteristics of the subjects are shown in Table 1. The study was performed in compliance with legal policy and ethical review boards for postmortem brain studies. Frozen sections (16 µm) were prepared with a cryostat at − 20 °C, thaw-mounted onto

Table 1 Demographic characteristics, postmortem delay (PMD), cause of death and brain pH of subjects included in the study

Subject	Gender	Age	PMD	Cause of death	Brain pH
1	Male	82	3	Natural/cardiorespiratory failure	ND
2	Female	57	11	Natural/hemorrhage	ND
3	Male	44	5	Natural/cardiorespiratory failure	6.2
4	Male	38	3	Natural/cardiorespiratory failure	6.2
5	Male	21	3	Accident/fall from height	6.34
6	Male	19	7	Accident/fall from height	6.7
7	Male	31	11	Homicide/knife wounds	6.53
8	Male	49	13	Accident/traffic	6.4
9	Male	71	8	Accident/fall from height	5.92
10	Male	21	35	Natural/cardiorespiratory failure	ND
11	Male	53	40	Homicide/gun wounds	ND
12	Male	35	41	Accident/drowning	ND

poly-L-lysine-coated glass slides (Superfrost Plus, Menzel Glaser, Braunschweig, Germany) and stored at − 80 °C until usage.

Radioactive ISH

We used radioactive ISH on mouse brain slices of the entire brain to determine the distribution of hevin and SPARC mRNA. Antisense oligonucleotide probes (35-mer) were designed to detect specifically mRNAs encoding mouse hevin (SPARCL1) and mouse SPARC (Table 2). All antisense probes were tested for specificity using BLAST (http://blast.ncbi.nlm.nih.gov/Blast.cgi). In situ hybridization was carried out as described previously (Vialou et al. 2007). The probes were 3′ end-labeled with [alpha-^{35}S] dATP (370 gigabecquerel/mmol; Perkin Elmer, Waltham, Massachusetts, USA) using terminal deoxynucleotidyl transferase (Roche Applied Biosystems, Nonnenwald, Germany) at a specific activity of 5×10^8 disintegrations per minute/µg. Sections were fixed in 3.7% formaldehyde in phosphate-buffered saline (PBS) for 1 h, washed in PBSX1, rinsed in water, dehydrated in 70% ethanol and air-dried. Hybridization was carried out at 42 °C for 16 h in hybridization medium (Oramacell, Paris, France) containing a mixture of labeled antisense oligonucleotides (4×10^5 counts per minute/100 µl each). Sections were washed to a final stringency of 0.5 SSC (7.5 mM sodium citrate, 75 mM NaCl, pH 7.0) at 53 °C, dehydrated in ethanol, air-dried and exposed to Fujifilm BioImaging Analyzer BAS-5000 (Fujifilm Life Science, Stamford, Connecticut, USA) for 15 days. Three different oligo-probes tested separately showed an identical distribution pattern, demonstrating the specificity of the approach (data not shown). The control procedure to confirm the specificity of ISH labeling using sense-radiolabeled probes gave no signal.

ISH image analysis

Digitized autoradiography scans (Fujifilm Life Science) were exported in TIFF format using MCID image analysis software (Imaging Research, St. Catharines, Ontario, Canada). Coronal brain sections from two male and two female C57BL6J mice (12 weeks old) spanning the entire brain (from olfactory bulbs to brainstem) were used. Around 45 sections with a step of 144 µm between two consecutive sections per mice were analyzed. Specific brain regions were identified according to the mouse brain atlas (Paxinos and Franklin 2001). A qualitative estimate of hevin mRNA intensity was assessed at the macroscopic level on digitized autoradiography scans as highest density (++++), high

Table 2 Oligonucleotides and cRNA probes used in present study. Gene symbol, common gene name, NCBI accession number, size and position are indicated

Probe	Gene symbol	Common gene name	NCBI accession #	Size (bp)	5′ Position
Oligonucleotide (ISH mouse)	*Sparcl1*	Hevin (mouse)	NM_010097	35	756, 1081, 1734
	Sparc	Sparc (mouse)	NM_009242	35	175, 753, 1300
cRNA (FISH mouse)	*Sparcl1*	Hevin (mouse)	NM_010097	1299	126
	Slc1a3	GLAST (mouse)	NM_148938	658	1350
	Slc17a7	VGLUT1 (rat)	NM_053859	508	115
	Slc17a6	VGLUT2 (mouse)	NM_080853	930	2315
	Gad1	GAD67 (rat)	NM_017007	539	195
	Pvalb	Parvalbumin (mouse)	NM_013645	517	74
	Calb1	Calbindin1 (mouse)	NM_009788	1122	268
	Cck	Cholecystokinin (mouse)	NM_031161	483	251
	Npy	Neuropeptide Y (mouse)	NM_023456	453	13
	Sst	Somatostatin (mouse)	NM_009215	401	143
	Chat	Choline acetyltransferase (rat)	NM_001170593	540	524
	Th	Tyrosine hydroxylase (rat)	NM_012740	998	456
	Tph	Tryptophane hydroxylase (mouse)	NM_009414	986	268
cRNA (FISH human)	*Sparcl1*	Hevin (human)	NM_001128310	908	1611
	Slc1a3	GLAST (human)	NM_004172.4	958	3113
	Slc17a7	VGLUT1 (human)	NM_020309	972	2082
	Gad1	GAD67 (human)	NM_000817	896	365
	Pvalb	Parvalbumin (human)	NM_002854.2	415	1

GAD67 glutamic acid decarboxylase 67, *GLAST* glutamate/aspartate transporter, *SPARC* secreted protein acidic and rich in cysteine, *VGLUT* vesicular glutamate transporter type

density (+++), moderate density (++), and low density (+) by considering signal strength. The intensity of the hevin signal was always within the linear range of the ^{14}C standard exposed together with the hybridized tissue. Representative sections were corrected for contrast and cropped using Photoshop CS6 (Adobe Systems, San Jose, California, United States), and assembled on Illustrator CS6 (Adobe Systems).

Double fluorescent ISH (FISH)

FISH was used to determine the phenotype of hevin-expressing cells in both mouse and human brain using probes of specific cellular markers (Table 2), as described previously (Apazoglou et al. 2018; Chazalon et al. 2018; Erdozain et al. 2018; Schweizer et al. 2014; Viereckel et al. 2016). Complementary RNA probes were synthesized with DIG- or fluorescein-labeled ribonucleoside tri-phosphate (Roche Applied Biosystems). The specificity of the probes was verified using NCBI blast. Cryosections were air-dried, fixed in 4% paraformaldehyde and acetylated in 0.25% acetic anhydride/100 mM triethanolamine (pH 8). Sections were hybridized for 18 h at 65 °C in 100 µl of formamide-buffer containing 1 µg/ml hevin digoxigenin-labeled riboprobe (DIG) and 1 µg/ml cell-marker fluorescein-labeled riboprobe for mouse sections and with hevin fluorescein-labeled riboprobe and DIG-labeled cell-marker riboprobe for human sections (Table 2). Sections were washed at 65 °C with SSC buffers of decreasing strength, and blocked with 20% fetal bovine serum and 1% blocking solution (Roche Applied Biosystems). Fluorescein epitopes were detected with horseradish peroxidase (HRP) conjugated anti-fluorescein antibody at 1:1000 and revealed with TSA kit (Perkin Elmer) using biotin-tyramide at 1:75 followed by incubation with Neutravidin Oregon Green conjugate at 1:750. HRP-activity was stopped by incubation of sections in 0.1 M glycine followed by a 3% H2O2 treatment. DIG epitopes were detected with HRP anti-DIG Fab fragments at 1:1000 and revealed with TSA kit (Perkin Elmer) using Cy3 tyramide at 1:200. Nuclear staining was performed with 4′ 6-diamidino-2-phenylindole (DAPI). The distribution of all probes is in agreement with those previously described in the mouse and human brain, confirming the reliability of our FISH procedures.

FISH image acquisition

All slides were scanned on a NanoZoomer 2.0-HT (Hamamatsu Photonics, Hamamatsu City, Japan) at 20x resolution. Laser intensity and time of acquisition was set separately for each riboprobe. Images were analyzed using the NDP.view2 software (Hamamatsu Photonics). Regions of interest were identified according to the Paxinos mouse brain atlas (Paxinos and Franklin 2001). Positive cells refer to a staining in a cell body clearly above background and surrounding a DAPI-stained nucleus. Co-localization was determined by the presence of the signals for both probes in the soma of the same cell. The entire region of interest was evaluated. For illustration purposes, the NanoZoomer images were exported in TIFF format using NDP viewer. Images were corrected for contrast, cropped on Photoshop CS6, and assembled on Illustrator CS6.

Results

Topographic expression of hevin mRNA in the adult mouse brain

First, we investigated the distribution of hevin transcript in adult mouse brain coronal sections using a mixture of three radiolabeled oligonucleotides (Table 2). As shown on film autoradiography, hevin mRNA was found throughout the brain with varying levels of intensity (Fig. 1a). Estimates of hevin mRNA expression levels in major brain structures are shown in Table 3. A strong expression was observed in cortical regions with the highest density in layers II/III and V of cortex; hippocampal subdivisions including presubiculum, and dentate gyrus; lateral and medial globus pallidus; and specific thalamic nuclei including anterodorsal thalamus, lateral habenula, laterodorsal thalamus, reticular thalamus, subthalamic nucleus, and zona incerta. Many nuclei in the midbrain and in the hindbrain contained a high density of hevin signal, including the dorsolateral geniculate, motor nuclei III and IV, red nucleus, superior and inferior colliculus; Bergman glial cells of cerebellum; and pontine reticular nucleus, reticulotegmental nucleus of the pons, superior olive nucleus, tegmental nucleus, and motor nuclei V, VII, X and XII in the hindbrain. Lower intensity of hevin mRNA expression was observed in the rest of brain, in particular in the anterior olfactory nucleus, striatum, CA1 and CA3 of the hippocampus, and the molecular layer of the cerebellum. Hevin mRNA was poorly expressed in the white matter. Fluorescent ISH with a DIG-labeled hevin cRNA probe in the mouse brain confirmed this regional pattern of expression (Figs. 2, 3, 4, 5, 6, 7, 8, 9, 10). The regional pattern of expression of hevin was similar in male and female mice at both 9 and 12 weeks old (data shown only for a 12-week-old male).

Hevin and its close homologue SPARC share 53% identity overall and 62% identity over their follistatin-like and calcium-binding domains, suggesting functional conservation of this region (Girard and Springer 1995). As shown on film autoradiography, SPARC mRNA showed a radically different distribution from that of hevin mRNA in mouse brains (compare Fig. 1b, a). SPARC mRNA was expressed at low levels, with little regional differences except in claustrum, vertical diagonal band, lateral globus pallidus, hypothalamus

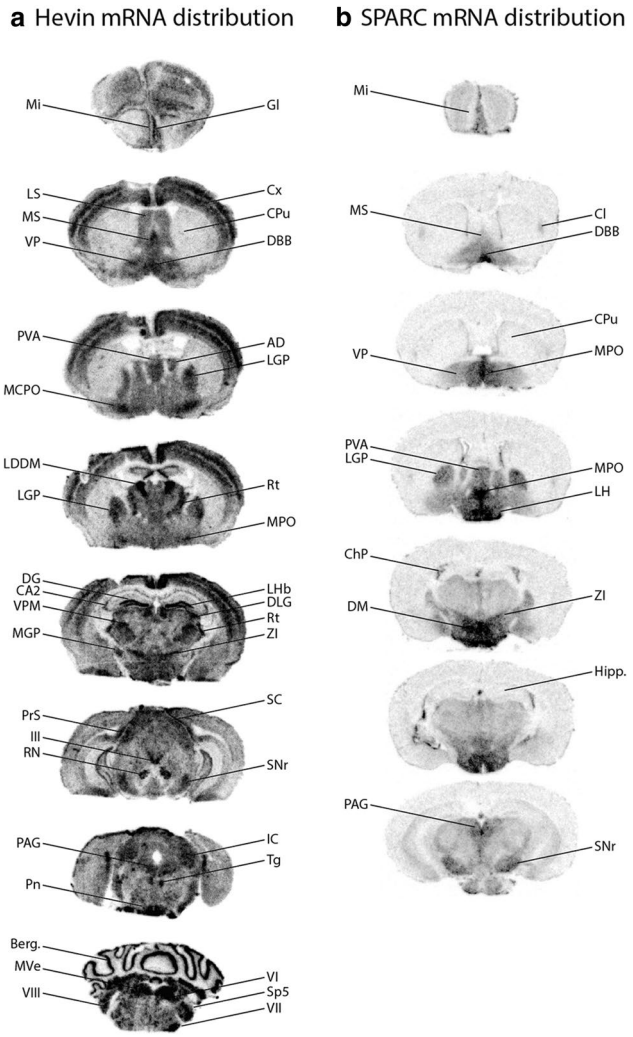

Fig. 1 Distribution of hevin and SPARC mRNA in adult mouse brain. **a** Autoradiograms of coronal brain sections labeled with oligonucleotide antisense ^{35}S-radiolabeled probes specific for mouse hevin. Hevin is strongly expressed in cortical layers II/III and V, reticular thalamus, anterodorsal thalamus, superior colliculus, motor nuclei III, VI, VII, VIII and cerebellum, and weakly expressed in the striatum (see Table 3 for hevin regional distribution). **b** Serial brain sections labeled with oligonucleotide antisense radiolabeled probes specific for SPARC in mouse brain. SPARC mRNA is expressed at low levels, but enriched in subcortical structures, in particular in the hypothalamus. See list of abbreviations

and substantia nigra pars reticulata, which showed high intensity levels.

Phenotypes of hevin mRNA-expressing cells in the adult mouse brain

Enrichment of hevin signal in specific brain structures suggests that different cellular populations may express hevin. To precisely identify the chemical phenotype of hevin-expressing cells, we used a DIG-labeled probe directed

Table 3 Relative densities of hevin mRNA expression in the mouse brain by ISH

Brain region	Intensity
Olfactory bulb	
Anterior olfactory nucleus	+
Glomerular layer	+++
Mitral cell layer	++
Cortex	
Layer I	++
Layer II–III	+++
Layer IV	++
Layer V	++
Layer VI	++
Hippocampus	
Granular layer of dentate gyrus	++++
Molecular layer of dentate gyrus	+
Polymorphic layer/Hilus	++
CA3 Pyramidal cell layer	+
CA3 Stratum oriens	+
CA3 Stratum radiatum	+
CA1 Pyramidal cell layer	+
CA1 Stratum oriens	+
CA1 Stratum radiatum	+
CA2 Pyramidal cell layer	+++
Presubiculum	++++
Subiculum	++
Septohippocampal nucleus	+
Septum	
Lateral septum	++
Medial septum	+++
Basal ganglia	
Caudate putamen	+
Lateral globus pallidus	++++
Medial globus pallidus	++++
Ventral pallidum	+++
Amygdala	
Basolateral amygdala	++
Central amygdala	++
Medial amygdaloid nucleus	++
Thalamus–hypothalamus	
Anterodorsal thalamic nucleus	++++
Anteroventral thalamic nucleus	++
Hypothalamus	+++
Thalamus–hypothalamus	
Interanteromedial thalamic nucleus	++
Lateral habenula	++++
Laterodorsal thalamic nucleus	++++
Mediodorsal thalamic nucleus	++
Paraventricular thalamic nucleus	+++
Subthalamic nucleus	++++
Reticular thalamic nucleus	++++
Ventral posteromedial thalamic nucleus	++

Table 3 (continued)

Brain region	Intensity
Zona incerta	++++
Midbrain	
Anterior pretectal nucleus	+++
Dorsal lateral geniculate nucleus	++++
Interpeduncular nucleus	++
Nucleus of Darkschewitsch	+++
Oculomotor nucleus (III)	++++
Periaqueductal gray	++
Prerubral field	++
Red nucleus	++++
Substantia nigra pars reticulata	+++
Superior colliculus	++++
Cerebellum	
Bergmann glial cells	++++
Molecular layer	+
Granule cell layer	+
Deep cerebellar nuclei	++
Pons	
Abducens nucleus (VI)	++++
Facial nucleus (VII)	++++
Gigantocellular reticular nucleus	+++
Lateral parabrachial nucleus	+++
Mesencephalic trigeminal nucleus	++
Motor trigeminal nucleus (V)	++++
Pontine reticular nucleus, oral part	++++
Principal sensory trigeminal nucleus	++++
Reticulotegmental nucleus of the pons	++++
Spinal trigeminal nucleus	++++
Superior olive nucleus	++++
Tegmental nucleus	++++
Vestibular nucleus	++++

Qualitative estimates of hevin mRNA expression were made based on the signal strength of the hybridization signal in a given structure. Rating scale for hevin mRNA labeling intensity: very high (++++), high (+++), moderate (++), low (+)

against hevin mRNA and fluorescein-labeled probes to detect mRNA encoding markers of astrocytes and various types of neurons (Table 2).

Astrocytes

We used the glutamate/aspartate transporter (GLAST), also known as excitatory amino acid transporter 1, a specific marker of astrocytes (Cahoy et al. 2008). We observed an almost complete co-localization of hevin with GLAST mRNA signals (arrowheads in Fig. 2). Accordingly, astrocytes in almost every brain region expressed hevin, as illustrated for cortex (Fig. 2a), striatum (Fig. 2b), lateral septum (Fig. 2c), hippocampus (Fig. 2d), hypothalamus (Fig. 2e) and cerebellum (Fig. 2f). Surprisingly, in two brain areas, the septohippocampal nucleus and the dorsal part of the lateral septum, both signals were detected, but did not co-localize (Fig. 2c). Hevin astrocytic expression across the entire brain is listed in Table 4.

In almost all brain regions, hevin was also expressed in a large portion of GLAST-negative cells (arrows in Fig. 2a–d), which is consistent with its neuronal expression (Kucukdereli et al. 2011; Lively and Brown 2008c; Lively et al. 2011; Lloyd-Burton and Roskams 2012; McKinnon et al. 2000; Mendis et al. 1996; Risher et al. 2014). Qualitatively, the staining in these GLAST-negative cells was different, i.e., a larger somatic staining surrounding the nucleus.

Neurons display a wide diversity of neurotransmitter content, projections, biophysical properties and functional roles and can be divided into excitatory glutamatergic neurons, inhibitory GABAergic neurons, and modulatory monoaminergic and cholinergic neurons. The regional distribution of these hevin-positive and GLAST-negative cells in several cortical layers, specific thalamic nuclei and other subcortical areas suggested that hevin could be expressed in both glutamatergic and GABAergic neurons. To test this hypothesis, we used markers of glutamatergic and GABAergic neuronal populations.

Glutamatergic neurons

The vast majority of neurons in the CNS are excitatory glutamatergic neurons that can be identified by the expression of the vesicular glutamate transporters VGLUT1 and VGLUT2. VGLUT1 and VGLUT2 transcripts allow the identification of cortical and subcortical glutamatergic neurons, respectively (Herzog et al. 2001). Overall, we identified three cellular populations: neurons that expressed both hevin and VGLUT mRNA (arrowhead in Fig. 3 for VGLUT1 and Fig. 4 for VGLUT2), non-glutamatergic cells that expressed hevin mRNA alone (arrow in Figs. 3, 4), and VGLUT-positive neurons that did not express hevin mRNA (star in Figs. 3, 4).

The proportion of each population varied between brain structures. In the cortex, hevin mRNA, which was distributed on cortical layers I to VI, co-localized with VGLUT1-mRNA across layers II to VI (arrowhead in Fig. 3a). In all layers, a substantial amount of hevin mRNA-expressing cells did not express VGLUT1 mRNA (arrow in Fig. 3a). In the hippocampus, hevin mRNA was found in glutamatergic granule cells of dentate gyrus, but was rarely visualized in pyramidal glutamatergic neurons of CA1-3 (Fig. 3b), as also evidenced by the weak signal in CA1-3 observed with ISH experiments (Fig. 1a; Table 3). In the olfactory bulb, hevin mRNA was observed in VGLUT1-positive glutamatergic neurons of mitral cell layer, but not in those of the anterior olfactory nucleus (Fig. 3c). In the cerebellum, hevin mRNA

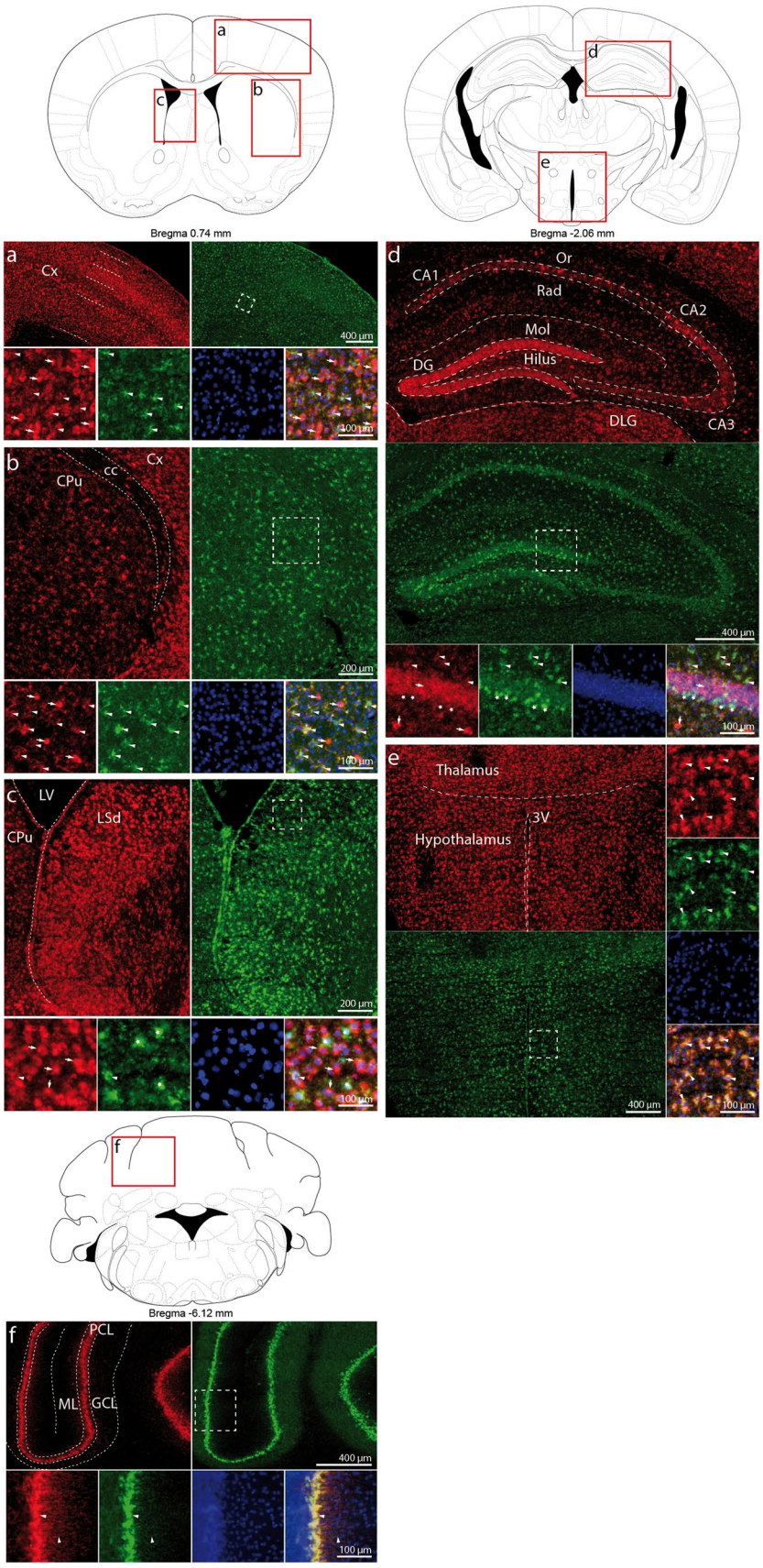

Fig. 2 Hevin mRNA is found in astrocytes expressing GLAST mRNA in mouse brain. At low magnification, hybridization signal for hevin (red) and GLAST (green) mRNA is observed throughout all regions of the brain, including cortex (**a**), striatum (**b**), lateral septum (**c**), hippocampus (**d**), hypothalamus (**e**), and cerebellum (**f**). At high magnification, photomicrographs show co-localization between hevin and GLAST (arrowhead) in each area. A substantial number of GLAST-negative cells express hevin mRNA (arrow) in cortex (**a**), striatum (**b**), lateral septum (**c**) and hippocampus (**d**), while in hypothalamus and cerebellum, hevin is found in astrocytes only (**e**, **f**). Hevin mRNA is absent from GLAST-positive astrocytes in the dorsal part of the lateral septum (star, **c**). Note that astrocytic hevin mRNA staining is somatic and is also present along glial processes in cerebellum (arrowhead, **f**) and that hevin is absent from progenitor cells in the subgranular layer of dentate gyrus, which express GLAST (star, **d**). DAPI signal is also presented (blue staining in the nucleus). See list of abbreviations

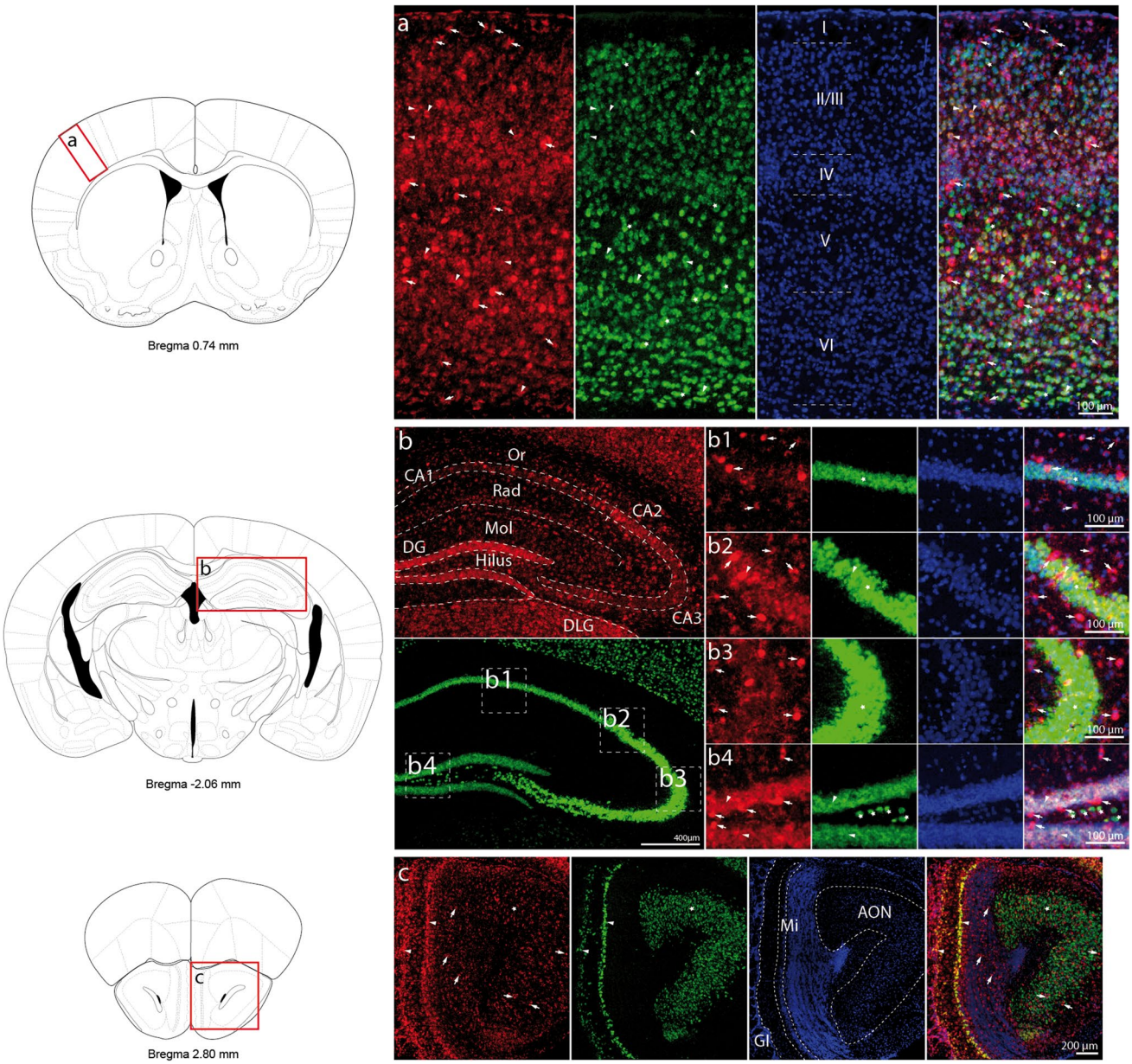

Fig. 3 Characterization of hevin mRNA expression in VGLUT1-positive glutamatergic neurons in mouse brain. Hybridization signal for hevin (red) and VGLUT1 (green) mRNA is observed in cortex (**a**), hippocampus (**b**) and olfactory bulb (**c**). a High-magnification images show only partial co-localization (arrowhead) in VGLUT1-positive glutamatergic neurons scattered throughout cortical layers II to VI. Neurons expressing only VGLUT1 mRNA (star) are also present. **b** In the hippocampus, hevin is expressed in glutamatergic granular neurons of the dentate gyrus (arrowhead, b4) and in a few glutamatergic pyramidal neurons of CA2 (b2). Hevin mRNA is absent from VGLUT1-positive neurons of CA1--CA3 and hilus of dentate gyrus (star, b1–b3). **c** In the olfactory bulb, hevin signal co-localizes with the VGLUT1-positive mitral cells (arrowhead) but not with VGLUT1-positive glutamatergic neurons of the anterior olfactory nucleus and glomerular layer (arrow). In addition to hevin staining in astrocytes identified by fine processes and small soma size, many cells expressing hevin mRNA do not co-localize with VGLUT1 mRNA in the three regions depicted here (arrow). DAPI signal is also presented (blue staining in the nucleus). See list of abbreviations

was absent from VGLUT1-positive glutamatergic neurons of the granular cell layer (not shown).

Subcortical areas expressed varying levels of hevin mRNA (Fig. 1a; Table 3). We found that hevin mRNA co-localized with VGLUT2 mRNA in several glutamatergic thalamic nuclei such as anterodorsal thalamus (Fig. 4a1), dorsal lateral geniculate (Fig. 4b1), ventral posteromedial thalamus (Fig. 4b2), subthalamus, and zona incerta (not shown). Hevin is also found in midbrain nuclei such as the dorsal part of periaqueductal gray (Fig. 4c1), red

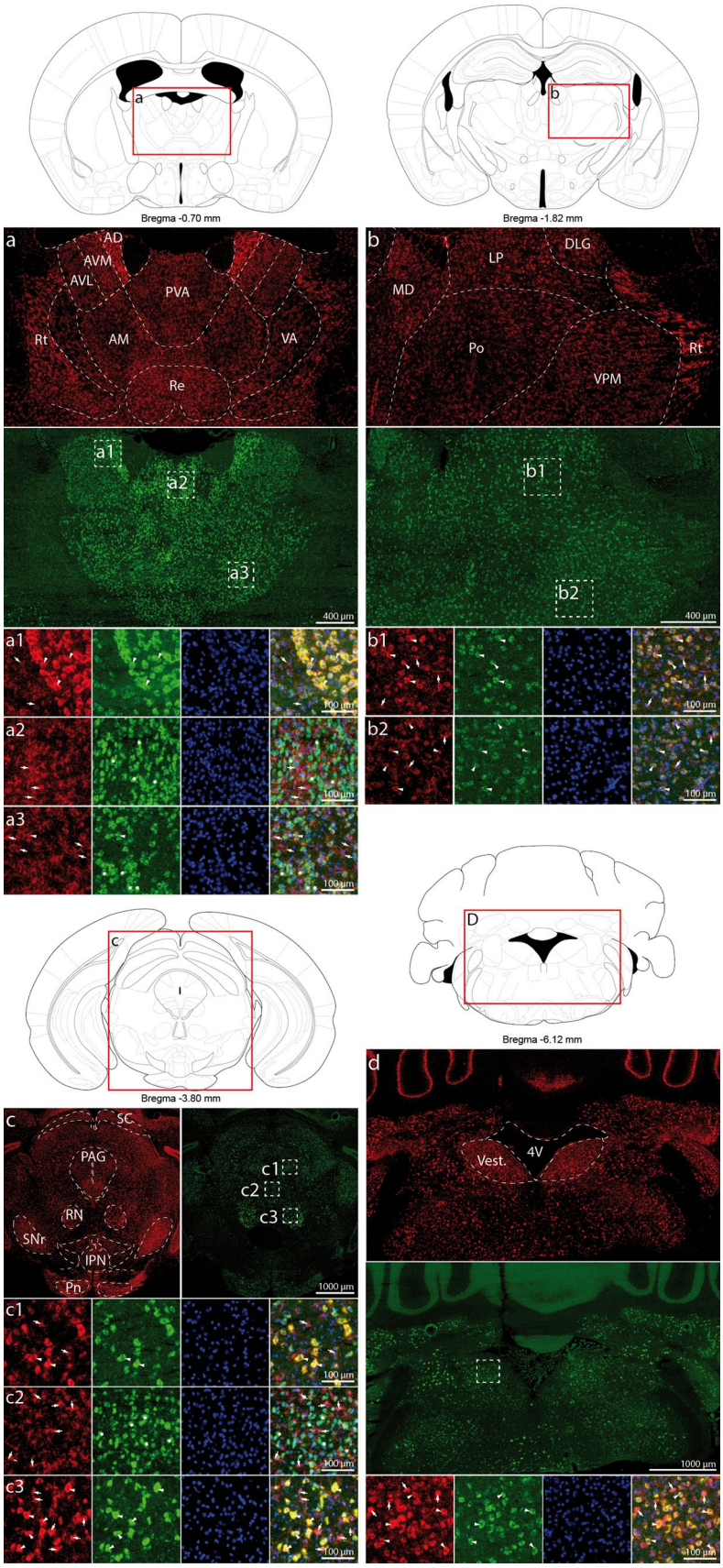

Fig. 4 Characterization of hevin mRNA expression in VGLUT2-positive glutamatergic neurons in mouse brain. Hybridization signal for hevin (red) and VGLUT2 (green) mRNA is observed in the thalamus (**a**, **b**) as well as in various nuclei of the hindbrain (**c**) and brainstem (**d**). Neurons expressing hevin mRNA in anterodorsal thalamus (a1), lateral posterior thalamus and dorsolateral geniculate (b1), ventral posteromedial thalamus (b2), periaqueductal gray (c1), red nucleus (c3) and vestibular nucleus (d1) are all VGLUT2-positive glutamatergic neurons (arrowhead). In other thalamic regions, hevin mRNA labeling (arrow) does not co-localize with VGLUT2 neurons (star), e.g., in paraventricular thalamus (a2), reuniens thalamus (a3), and nucleus of Darkschewitsch (c2). Cells expressing hevin mRNA are observed in reticular thalamic nucleus, which is devoid of VGLUT2-positive neurons (**a**). DAPI signal is also presented (blue staining in the nucleus). See list of abbreviations

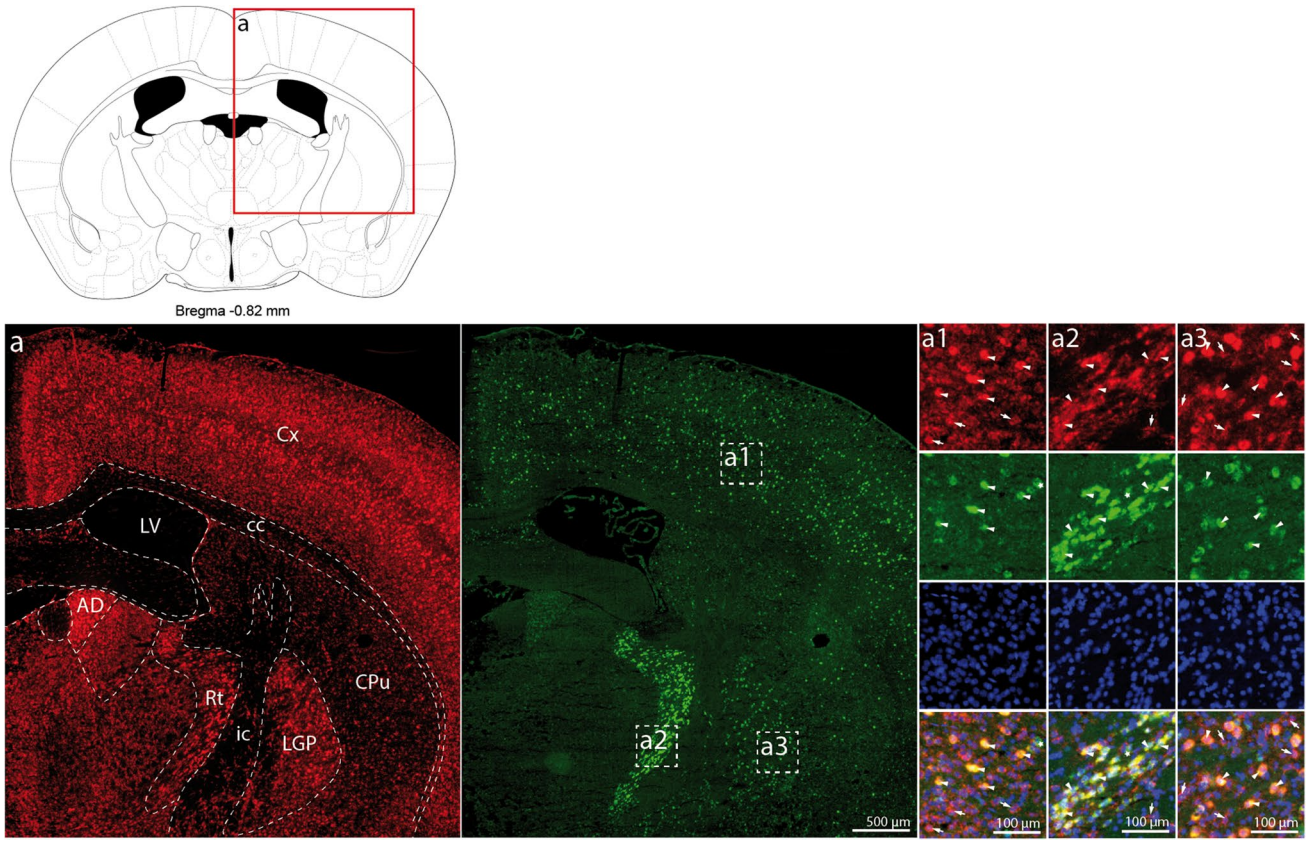

Fig. 5 Characterization of hevin mRNA expression in GABAergic neurons expressing GAD67 mRNA in mouse brain. Hybridization signal for hevin (red) and GAD67 (green) mRNA is observed in the cortex (a1), reticular thalamus (a2), and lateral part of the globus pallidus (a3). High-magnification images show an almost complete co-localization between hevin and GAD67 mRNAs (arrowhead, a1–a3). A small number of GAD67 neurons do not express hevin (star, a1, a2). In the cortex, a majority of hevin-positive cells do not co-localize with GAD67 mRNA signal (arrow, a1–a3). DAPI signal is also presented (blue staining in the nucleus). See list of abbreviations

nucleus (Fig. 4c3), interpeduncular nucleus, and prerubral field (not shown), and nuclei in the pons such as the vestibular nucleus (Fig. 4d). Despite the clear co-localization of hevin and VGLUT2 in these nuclei, hevin was absent from VGLUT2-positive neurons in many other brain regions, e.g., paraventricular thalamus (Fig. 4a2), ventral anterior thalamus (Fig. 4a3), and ventral part of periaqueductal gray (Fig. 4c2). In the hypothalamus, hevin mRNA was only expressed in astrocytes, except in the lateral mammillary nucleus, where hevin co-localized with VGLUT2-positive neurons (not shown). In regions where hevin was expressed only in some glutamatergic neurons, dual labeled cells did not delineate any neuroanatomical boundary, as they were randomly intermingled with hevin-negative glutamatergic neurons. See Table 4 for a summary of the co-localization between hevin and VGLUT1 and VGLUT2 mRNA across the mouse brain.

GABAergic neurons

Throughout the brain, many cells expressing hevin mRNA did not co-localize with GLAST (arrows in Fig. 2a–d), VGLUT1 (arrows in Fig. 3a–c) or VGLUT2 mRNAs (arrows in Fig. 4a–d), suggesting that GABAergic inhibitory neurons express hevin mRNA. Double FISH experiments performed to detect hevin and GAD67 (also called GAD1, glutamic acid decarboxylase) mRNAs, a marker of GABAergic neurons, showed an almost complete co-localization in the cortex (Fig. 5a1), reticular thalamus (Fig. 5a2), and lateral globus pallidus (Fig. 5a3). GABAergic neurons, which are the major source of inhibitory input in CNS, display a wide diversity of morphologies, biophysical properties, molecular markers and functional roles (Mendez and Bacci 2011; Tepper et al. 2010). To further characterize the phenotype of hevin-positive

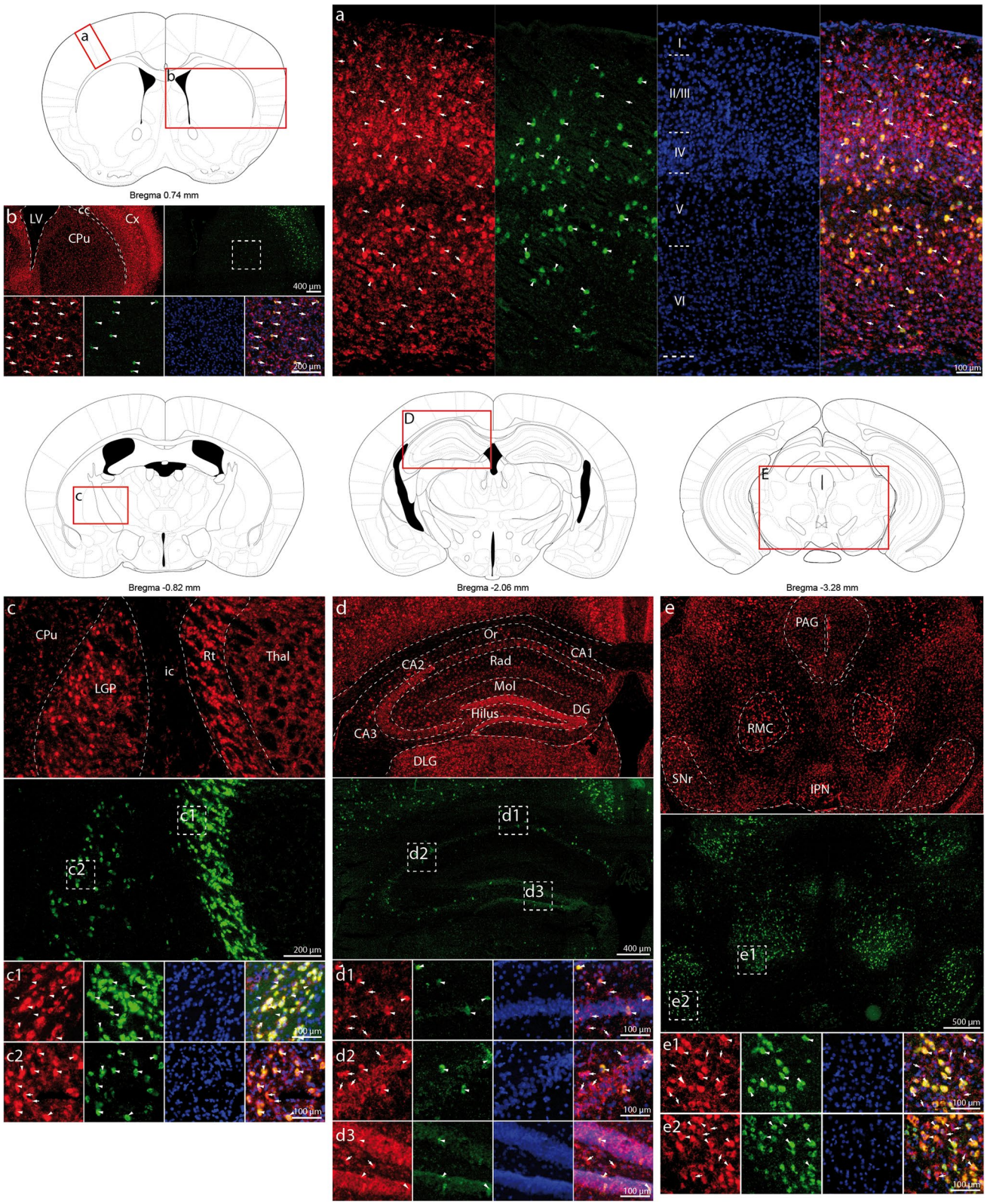
a
b
Bregma 0.74 mm
LV
cc
Cx
CPu
400 µm
200 µm
I
II/III
IV
V
VI
100 µm
c
Bregma -0.82 mm
D
Bregma -2.06 mm
E
I
Bregma -3.28 mm
CPu
LGP
ic
Rt
Thal
c1
c2
200 µm
Or
CA2
Rad
CA1
Mol
Hilus
DG
CA3
DLG
d1
d2
d3
400 µm
PAG
RMC
SNr
IPN
e1
e2
500 µm
100 µm

◂**Fig. 6** Hevin mRNA is expressed in parvalbumin neurons and neurons in mouse brain. Hybridization signal for hevin (red) and parvalbumin (green) mRNA is observed throughout the brain, including cortex (**a**), striatum (**b**), reticular thalamus (c1), lateral globus pallidus (c2), hippocampus (**d**), and several midbrain nuclei (**e**). High-magnification images show a complete co-localization between hevin and parvalbumin mRNAs in these regions (arrowhead, a–e). All parvalbumin-positive interneurons express hevin mRNA in layers II to VI of cortex (**a**), striatum (**b**), all hippocampal subfields, substantia nigra (e2), and red nucleus (e1). All parvalbumin-positive projection neurons in reticular thalamic nucleus (c1) and lateral globus pallidus (c2) express hevin mRNA. As expected, hevin mRNA is also observed in non-parvalbumin interneurons in cortex (**a**), CA2 (d2) and dentate gyrus (d3) (arrow). DAPI signal is also presented (blue staining in the nucleus). See list of abbreviations

GABAergic neurons, we used well-validated molecular markers of these neurons (Table 2).

Based on hevin mRNA strong expression in the mouse globus pallidus and reticular thalamic nucleus (Figs. 1a, 5), two parvalbumin-enriched nuclei, we hypothesized that hevin would be present specifically in parvalbumin-expressing projection neurons. In the globus pallidus and reticular thalamic nucleus, parvalbumin neurons project to substantia nigra pars reticulata and various thalamic nuclei, respectively (Clemente-Perez et al. 2017). In the rest of the brain, the majority of parvalbumin-expressing cells are local interneurons. We found that distribution of parvalbumin mRNA paralleled hevin mRNA in the entire brain (Fig. 6). Hevin and parvalbumin transcripts co-localized in almost all brain regions studied, including cortex (Fig. 6a), striatum (Fig. 6b), reticular thalamus (Fig. 6c1), lateral globus pallidus (Fig. 6c2), hippocampus (Fig. 6d), red nucleus (Fig. 6e1), and substantia nigra pars reticulata (Fig. 6e2). Surprisingly, in the cerebellum, hevin was absent

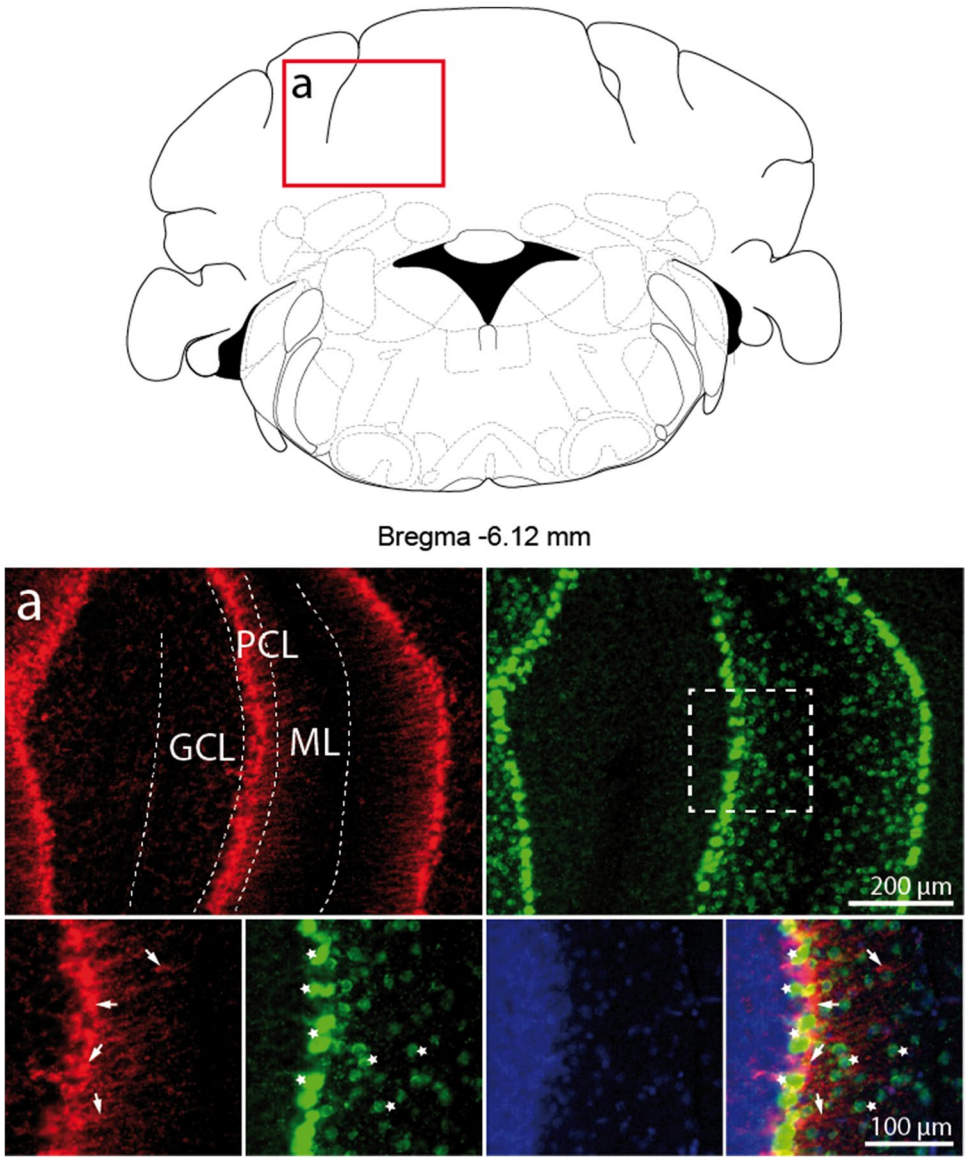

Fig. 7 Absence of hevin mRNA in parvalbumin-positive interneurons and Purkinje cells of cerebellum in mouse brain. Hybridization signal for hevin (red) and parvalbumin (green) mRNA is observed in cerebellum. a In the Purkinje cell layer, hevin is expressed only in Bergman glial cells (see Fig. 3e) that surround parvalbumin-positive neurons (star). Parvalbumin interneurons in the molecular layer do not express hevin mRNA (star). DAPI signal is also presented (blue staining in the nucleus). See list of abbreviations

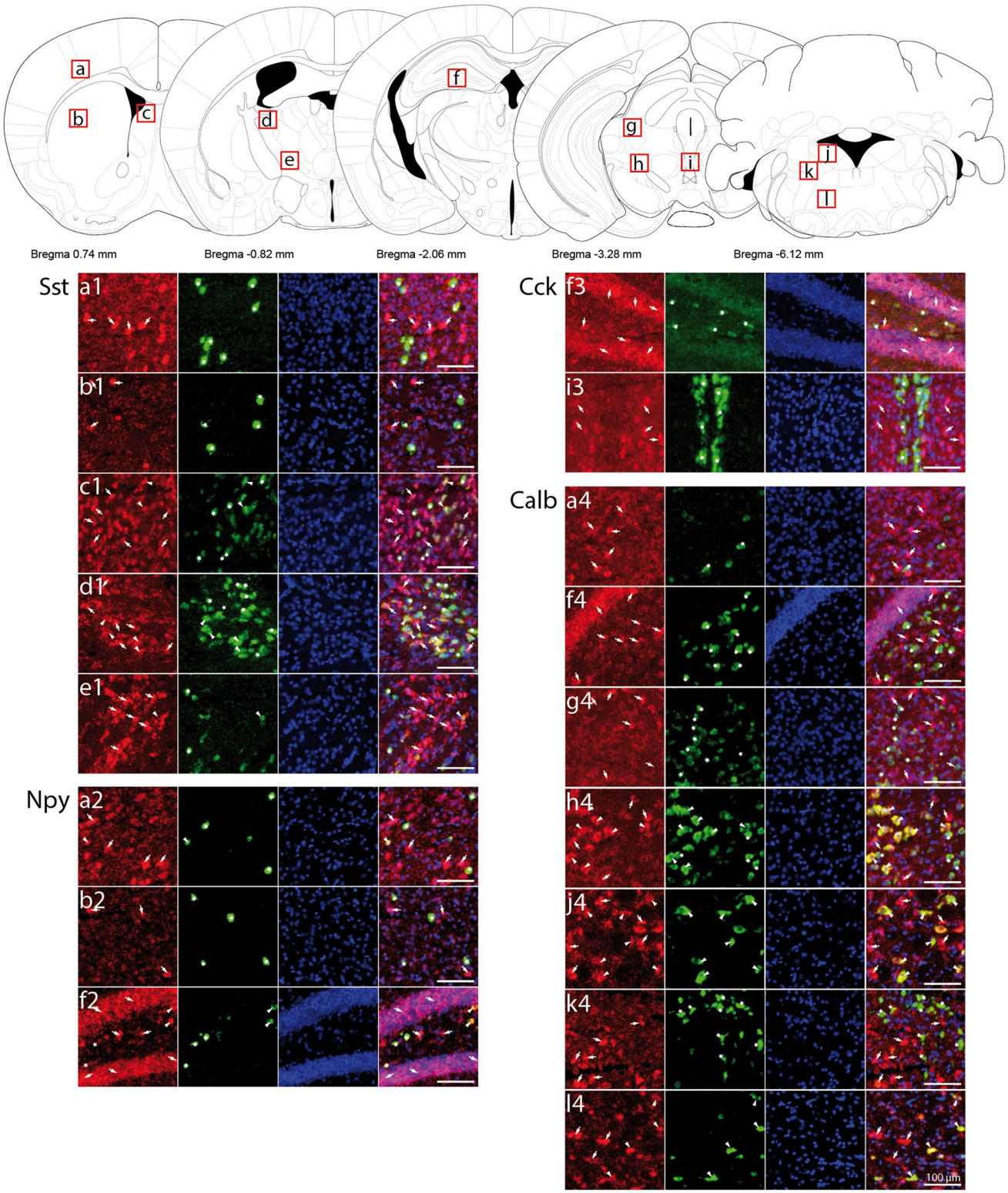

from parvalbumin-positive Purkinje cells and interneurons of the molecular layer (star in Fig. 7). Using cell type-specific mRNA ribosomal purification, we confirmed the lack of hevin mRNA expression in parvalbumin-positive neurons of the cerebellum (Supplementary Fig. 1). In contrast, qRT-PCR revealed enrichment in hevin mRNA in parvalbumin-positive neurons of dorsal striatum and hippocampus (Supplementary Fig. 2). Likewise hevin mRNA was enriched after ribosomal purification in astrocytes of hippocampus (Fig. S2). These results suggest that hevin mRNA

◂**Fig. 8** Characterization of hevin mRNA in GABAergic neurons expressing somatostatin, neuropeptide y, cholecystokinin and calbindin mRNAs in mouse brain. Hybridization signal for hevin (red) and somatostatin (1), neuropeptide Y (2), cholecystokinin (3) and calbindin (4) mRNA (green) is observed throughout the brain, including cortex (**a**), striatum (**b**), lateral septum (**c**), reticular thalamus (**d**, **e**), dentate gyrus (**f**), anterior pretectal nucleus and deep mesencephalic nucleus (**g**), posterior thalamic nuclear group (**h**), Edinger–Westphal nucleus (**i**), vestibular nucleus (**j**), parvicellular reticular nucleus (**k**), and gigantocellular reticular nucleus (**l**). Somatostatin-positive neurons only co-localize with hevin mRNA in some regions (arrowheads, c1–e1). The majority of hevin-positive cells are negative for somatostatin mRNA labeling (arrow, a1–e1). Similarly, a large number of somatostatin-positive neurons do not express hevin mRNA (stars, a1–e1). Some co-localization is observed between hevin and neuropeptide Y mRNAs in the cortex and hippocampus (arrowhead, a2, f2). Most neuropeptide Y-positive cells in the cortex, striatum and dentate gyrus do not express hevin (stars, a2, b2, f2). In the dentate gyrus (f3) and the Edinger–Westphal nucleus (i3), no co-localization is observed between hevin-positive cells (arrows) and cholecystokinin-positive neurons (stars). Partial co-localization is observed between calbindin and hevin mRNAs in the hindbrain and brainstem (arrowhead, h4, j4, and l4). In the cortex (a4), dentate gyrus (f4), and dorsal midbrain (g4), no co-localization is observed (arrow for hevin mRNA and star for calbindin mRNA). DAPI signal is also presented (blue staining in the nucleus). The scale bar is 100 µm. *Calb* calbindin, *Cck* cholecystokinin, *NPy* neuropeptide Y, *Sst* somatostatin

is being translated into protein in both parvalbumin neurons and astrocytes.

In addition to parvalbumin, we used four common molecular markers of GABAergic neurons: somatostatin, neuropeptide Y, cholecystokinin, and calbindin, which segregate from parvalbumin-positive neurons, in particular in the cortex and hippocampus (Zeisel et al. 2015). The vast majority of somatostatin-positive neurons were sparsely distributed in cortex, hippocampus, striatum, lateral septum, basal nucleus, dorsal portion of reticular nucleus, periventricular hypothalamic areas, lateral geniculate nucleus, and few nuclei in brainstem, consistent with the reported distribution (Johansson et al. 1984). Almost all somatostatin-expressing neurons were negative for hevin mRNA, illustrated in the cortex (Fig. 8a1), striatum (Fig. 8b1), and ventral reticular thalamus (Fig. 8e1). However, hevin mRNA was found in some somatostatin-positive neurons in the lateral septum (Fig. 8c1), reticular thalamus (Fig. 8d1), parabrachial nucleus, reticulotegmental nucleus of the pons, and the oral part of the pontine reticular nucleus (not shown).

Neuropeptide Y-positive neurons were scattered in cortex, hippocampus, and striatum, and were almost nonexistent in thalamus, hypothalamus, midbrain, cerebellum, and brainstem, in agreement with their known distribution (Chronwall et al. 1985). Hevin mRNA was found in few neuropeptide Y-positive neurons: in layer II to VI of the cortex (Fig. 8a2), in the dentate gyrus (Fig. 8f2), CA3 region of hippocampus, basolateral amygdala, and medial amygdaloid nucleus (not shown).

Cholecystokinin-positive neurons were mostly found in cortex, amygdala, olfactory bulb, hippocampus, several thalamic nuclei, geniculate nucleus and substantia nigra compacta, and were almost absent in striatum, cerebellum and brainstem, as previously described (Savasta et al. 1988). Hevin mRNA was expressed only in cholecystokinin-positive neurons in the mitral cell layer of the olfactory bulb, anterior olfactory nucleus, and laterodorsal thalamic nucleus (not shown). No co-localization was observed in the hippocampus (Fig. 8f3), Edinger–Westphal nucleus (Fig. 8i3), cortex, nuclei of the basal ganglia complex, and amygdala (not shown).

Calbindin-positive neurons were distributed throughout the brain and found in olfactory bulb, cortex, hilus of dentate gyrus, lateral and medial septum, basal nucleus, thalamic and hypothalamic nuclei, midbrain and hindbrain nuclei. This expression pattern is consistent with published reports (Celio 1990). In all these regions, hevin mRNA was only present in calbindin-expressing neurons in the posterior thalamic nuclear group (Fig. 8h4), vestibular nucleus (Fig. 8j4), mesencephalic trigeminal nucleus (Fig. 8k4), reticulotegmental nucleus of the pons (Fig. 8l4) and principal sensory trigeminal nucleus (not shown). Hevin mRNA was also found in some calbindin interneurons of CA3 and CA1 layers of hippocampus (Fig. 8f4), inferior colliculus, and anterior pretectal nucleus (Fig. 8g4), and mostly absent in calbindin interneurons of the cortex (Fig. 8a4), olfactory bulb, striatum and all other thalamic, hypothalamic, midbrain and hindbrain nuclei (not shown). See Table 4 for a summary of the co-localizations between hevin mRNA and each marker of GABAergic neuron subtype.

Cholinergic neurons

In situ hybridization revealed that hevin was strongly expressed in the brainstem, in particular in motor nuclei (Fig. 1a). These nuclei are composed of large cholinergic neurons identifiable with the marker choline acetyltransferase (ChAT). We found that ChAT-positive neurons were distributed mostly in subcortical structures in the basal forebrain, midbrain and brainstem, in agreement with previous publications (Armstrong et al. 1983). Hevin mRNA co-localized with ChAT in all cholinergic neurons of motor nuclei III (Fig. 9C), IV, V (Fig. 9d), VI, VII (Fig. 9f) and XII (Fig. 9g), but not in cholinergic neurons of motor nuclei X and nucleus ambiguus (Fig. 9g). In contrast, in the midbrain and forebrain, hevin was absent from all cholinergic neurons, including the lateral tegmental nucleus (Fig. 9e), pedunculopontine tegmental nucleus and basal forebrain (Fig. 9a1, b), which comprises the nucleus of the diagonal band, the magnocellular preoptic nucleus, the substantia innominata and

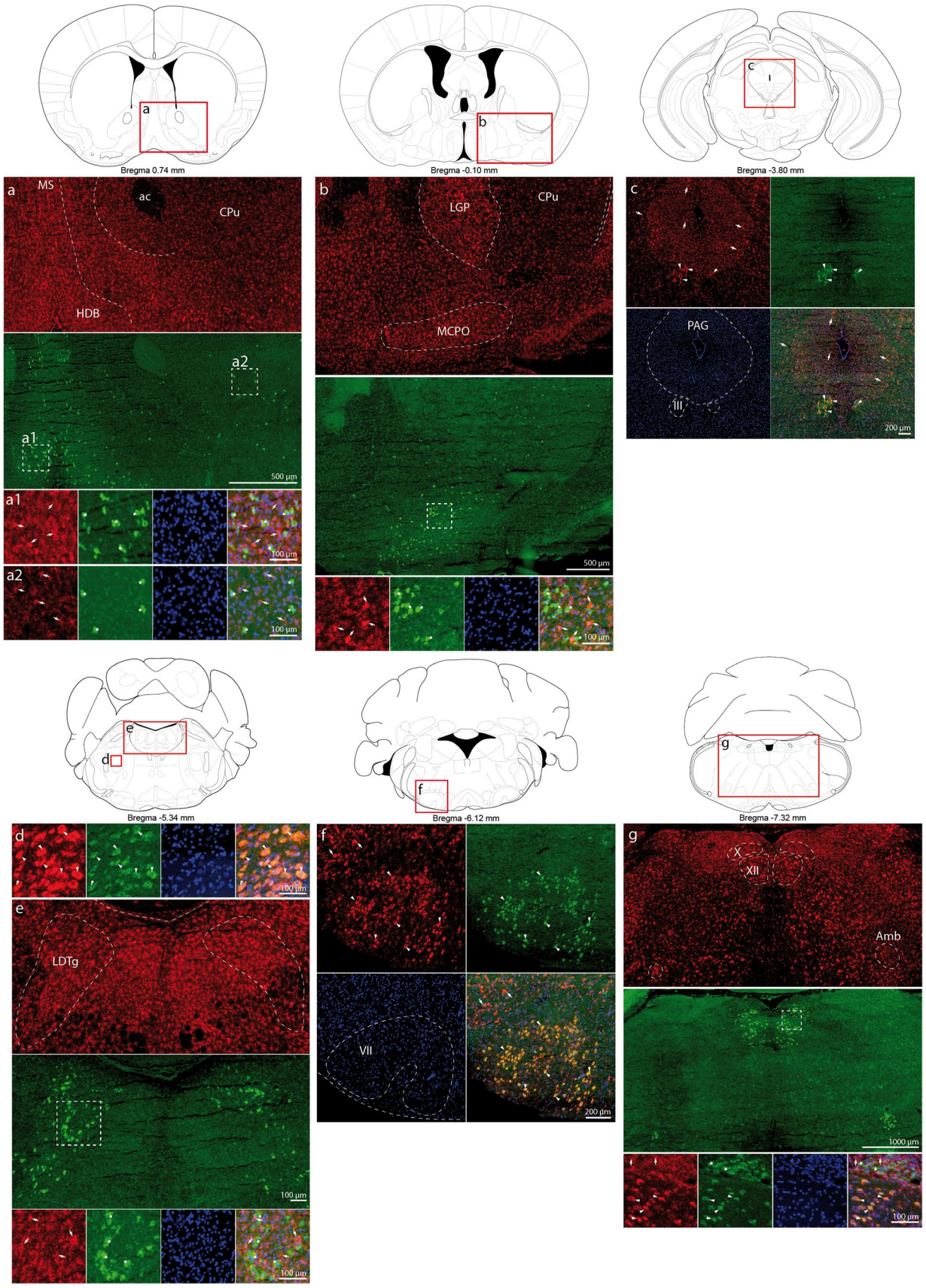
a
Bregma 0.74 mm
b
Bregma -0.10 mm
c
Bregma -3.80 mm
MS
ac
CPu
HDB
a2
a1
500 µm
100 µm
LGP
MCPO
PAG
III
200 µm
d
e
Bregma -5.34 mm
f
Bregma -6.12 mm
g
Bregma -7.32 mm
LDTg
VII
X
XII
Amb
1000 µm

◂**Fig. 9** Characterization of hevin mRNA in cholinergic neurons expressing choline acetyltransferase in mouse brain. Hybridization signal for hevin (red) and choline acetyltransferase (green) is observed throughout the brain including diagonal band of Broca and striatum (**a**), basal nucleus (**b**), motor nucleus III (**c**), laterodorsal tegmentum (**d**), motor nuclei V (**e**), VII (**f**), X, XII and Ambiguus (**g**). High-magnification images show total co-localization between ChAT-positive neurons in motor nuclei III, V, VII and XII and hevin mRNA signal (arrowhead). In all other cholinergic neurons, hevin mRNA labeling (arrow) does not co-localize with ChAT mRNA labeling (star), e.g., in cholinergic neurons of the forebrain as well as motor nuclei X and Ambiguus. DAPI signal is also presented (blue staining in the nucleus). The scale bar is 100 µm. See list of abbreviations

the globus pallidus. Cholinergic interneurons in the striatum were also negative for hevin (Fig. 9a2).

Monoaminergic neurons

The regional distribution of hevin mRNA showed that it was not enriched in monoaminergic nuclei, i.e., substantia nigra, ventral tegmental area, raphe nucleus and locus cœruleus (Fig. 1). We thus hypothesized that hevin was absent from monoaminergic neurons. We used tyrosine hydroxylase as a specific marker of catecholaminergic neurons and tryptophane hydroxylase type 2 as a specific marker of serotoninergic neurons. No co-localization was observed between hevin and tyrosine hydroxylase in the substantia nigra pars compacta, ventral tegmental area (star in Fig. 10a), and locus cœruleus (star in Fig. 10b), demonstrating that hevin mRNA is absent from dopaminergic and noradrenergic neurons. Likewise, in raphe nuclei, hevin mRNA did not co-localize with tryptophane hydroxylase 2 (star in Fig. 10c), showing that hevin is also absent from serotoninergic neurons.

Phenotypes of hevin mRNA-expressing cells in adult human prefrontal cortex and caudate nucleus

To determine if the specific cellular profile of hevin mRNA expression was conserved in the human brain, we performed double FISH on postmortem prefrontal cortical and caudate samples using GLAST, GAD67, PV, and VGLUT1, as markers for astrocytes, GABAergic, parvalbumin, and glutamatergic neurons, respectively. A similar pattern was observed between the different subjects. In the prefrontal cortex, hevin mRNA was present in most astrocytes (arrowhead in Fig. 11a), GABAergic neurons (arrowhead in Fig. 11b), and more specifically in parvalbumin neurons (arrowhead in Fig. 11c). In the human cortex, hevin mRNA was also expressed in glutamatergic neurons (arrowhead in Fig. 11d). A number of VGLUT1-positive neurons did not express hevin (star, Fig. 11d), showing that hevin expression is not specific to glutamatergic neurons in the human prefrontal cortex. Interestingly, hevin was differentially distributed in cortex (Fig. 11e), as observed in the mouse. In the caudate nucleus, hevin mRNA was expressed in astrocytes (arrowhead in Fig. 12a) and parvalbumin interneurons (arrowhead in Fig. 12b).

Discussion

In contrast to other matricellular proteins, hevin is strongly expressed in the adult brain, both in rodents (Hambrock et al. 2003; Johnston et al. 1990; McKinnon et al. 2000; Soderling et al. 1997) and humans (Girard and Springer 1995). The present study provides the first detailed description of hevin distribution in the brain and its expression in phenotypically identified neuron subtypes (summarized in Fig. 13). We did not identify any brain region that did not express hevin. This extensive expression of hevin throughout all brain regions is explained by its ubiquitous expression in astrocytes. Overall, our results reveal that hevin cellular phenotype in the brain is highly heterogeneous. Depending on the brain structure, hevin will be primarily present in astrocytes, parvalbumin neurons, other GABAergic inhibitory neuron subtypes, glutamatergic neurons, cholinergic motor neurons, or a combination of these cell types. Importantly, we show that hevin cellular expression profile is similar in the prefrontal cortex and caudate nucleus between mouse and human, suggesting a conserved cellular specificity between the two species. Whether this observation can be extended to other brain areas remains to be established in future studies. Furthermore, despite similarities in mRNA expression, hevin translation might also be differentially regulated between human and mouse, leading to differences in protein level. Our regional distribution study in mice reveals a strong expression for hevin in the cortex, hippocampus, basal ganglia complex, diverse thalamic nuclei and in cholinergic motor neurons in the brainstem. The discrete and specific distribution of hevin mRNA suggests that hevin might be involved in the synaptic plasticity underlying hippocampal-dependent processes such as learning and memory, and cortico-basal ganglia-thalamo-cortical loop processes such as goal-directed behaviors, decision-making and fine motor control.

Hevin neuronal expression has been overlooked in previous studies, overshadowed by its expression in almost all astrocytes, which represent nearly half of brain cells (Herculano-Houzel 2014; Markiewicz and Lukomska 2006; Nedergaard et al. 2003). Transcriptome studies using fluorescence-activated cell sorting or bacterial artificial chromosome-translating ribosome affinity purification analysis missed the discrete but strong neuronal expression profile of hevin (Cahoy et al. 2008; Morel et al. 2017). In addition to its widespread expression in astrocytes, we show here that hevin mRNA is remarkably and consistently observed in one GABAergic neuronal subtype, parvalbumin-expressing

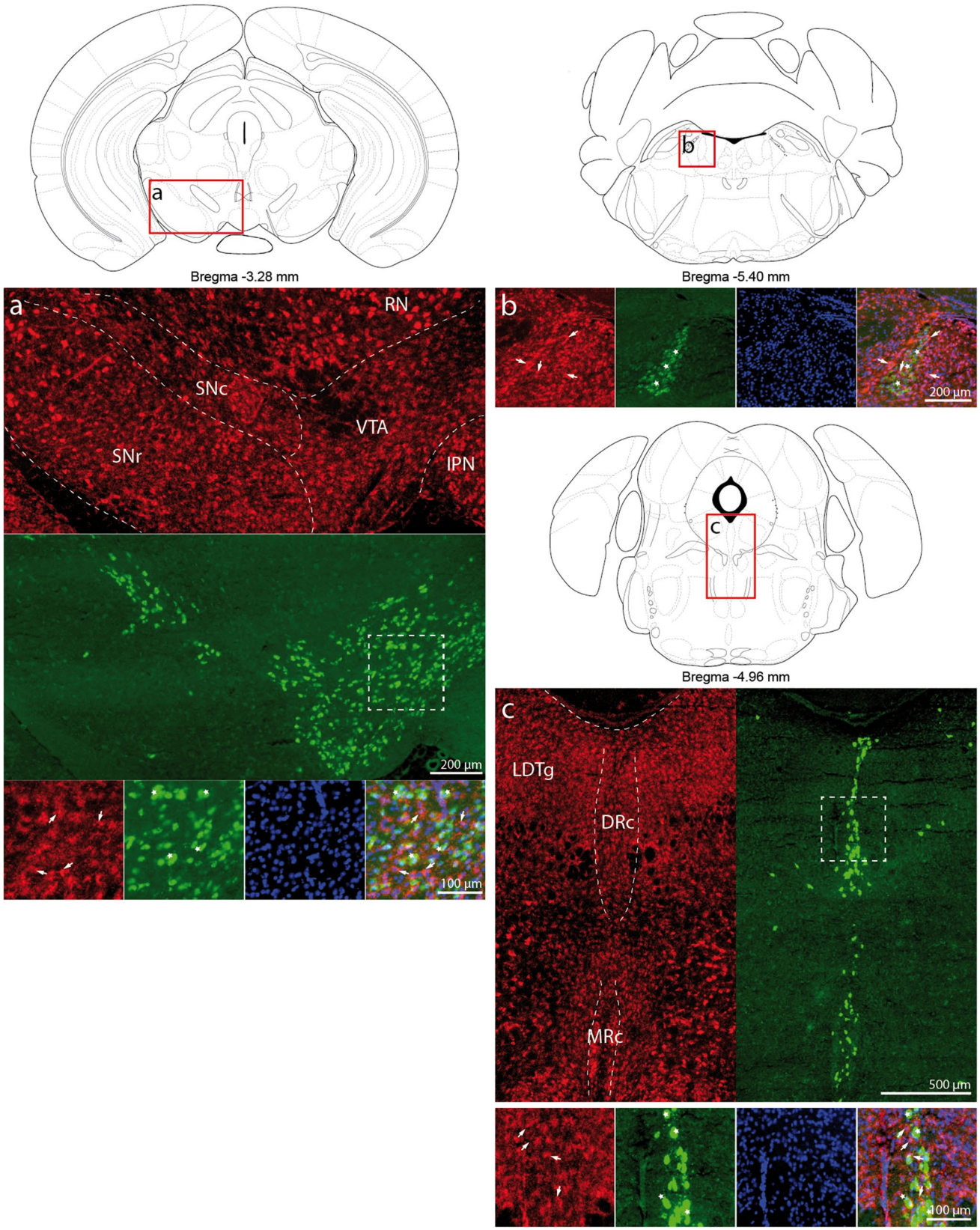
a
Bregma -3.28 mm
b
Bregma -5.40 mm
RN
SNc
VTA
SNr
IPN
200 µm
100 µm
200 µm
c
Bregma -4.96 mm
LDTg
DRc
MRc
500 µm
100 µm

◂**Fig. 10** Absence of hevin mRNA in monoaminergic nuclei in mouse brain. Hybridization signal for hevin (red) and tyrosine hydroxylase (green) is observed in midbrain monoaminergic nuclei, substantia nigra, ventral tegmental area (**a**), and locus cœruleus (**b**). Hybridization signal between hevin (red) and tryptophane hydroxylase (green) is observed in Raphe nuclei (**c**). No co-localization is observed between hevin-positive cells (arrows) and tyrosine hydroxylase-positive and tryptophane hydroxylase-positive neurons (stars). DAPI signal is also presented (blue staining in the nucleus). The scale bar is 100 µm. See list of abbreviations

projection neurons and parvalbumin-expressing local interneurons. As a result, in the mouse brain, hevin mRNA is robustly found in the reticular thalamus and lateral globus pallidus, and in the substantia nigra pars reticulata, regions of high density of long-range projection neurons, and local inhibitory interneurons, respectively. Hevin was also found to be expressed in a restricted number of other subpopulations of GABAergic neurons expressing calbindin, somatostatin, neuropeptide Y and cholecystokinin mRNA, compared to parvalbumin-expressing neurons. Additionally, hevin mRNA was abundantly found in subgroups of glutamatergic neurons in cortical and subcortical structures, as well as cholinergic neurons of brainstem motor nuclei. A recent study showed that, in humans, hevin protein is expressed in large neurons of the IIIrd, Vth, VIth, VIIth, IXth, Xth, XIth, XIIth motor nuclei in the brainstem and spinal cord (Hashimoto et al. 2016). This corroborates our observation of strong hevin expression in cholinergic neurons of motor nuclei in mouse, except in motor nucleus X and nucleus ambiguus, where hevin was only expressed in astrocytes.

To evaluate the singularity of hevin mRNA distribution compared to other matricellular proteins, we determined the distribution of SPARC mRNA. Our study shows radically different distributions for SPARC and hevin mRNAs. SPARC specific expression in glial cell types (Mendis et al. 1995; Vincent et al. 2008) matches the regional distribution of the astrocyte marker GLAST in the rodent brain, in accordance with higher density of astrocytes in the lateral septum, medial preoptic area, and hypothalamus (Cui et al. 2016; Emsley and Macklis 2006; Schmitt et al. 1997). Expression of both hevin and SPARC in astrocytes and the absence of obvious phenotypes in SPARC or hevin knockout mice have suggested that the two proteins might compensate for each other (Brekken and Sage 2000). However, their opposite effects on synaptogenesis (Jones et al. 2011; Kucukdereli et al. 2011), and on inflammatory processes (Blakely et al. 2015), and as shown here, their strikingly different regional and cellular brain distribution, suggest a peculiar role for hevin in adult CNS.

Implications for the role of hevin in the adult brain

The mRNA expression profile determined here is coherent with the distribution of hevin protein previously defined in both the mouse (Kucukdereli et al. 2011; Lively and Brown 2008c; Lively et al. 2011; Lloyd-Burton and Roskams 2012; McKinnon et al. 2000; Mendis et al. 1996; Risher et al. 2014) and the human (Hashimoto et al. 2016) brain. Additionally, our study reveals the phenotypic heterogeneity of the cells expressing hevin mRNA in both species. Hevin was previously detected in GFAP-positive astrocytes and in small subsets of NeuN-positive neurons in mouse hippocampus and cortex (Lloyd-Burton and Roskams 2012; Risher et al. 2014), suggesting that its mRNA is translated in at least some cell types and brain regions. To directly test this hypothesis, we used cell-type-specific isolation of mRNAs bound to tagged-ribosomes in mice (Ingolia et al. 2009) to challenge whether hevin was actively translated in parvalbumin neurons and astrocytes in mice, two cell types with consistent hevin mRNA expression. These experiments confirmed that hevin mRNA is actively translated in astrocytes and demonstrated its translation in parvalbumin interneurons of hippocampus and striatum, reinforcing the significance of our study and suggesting that the protein hevin may play a role in these cells in the adult brain. Hevin in astrocytes was shown to be required for synaptic stabilization of excitatory synapses, as well as for synaptic refinement during development (Risher et al. 2014; Singh et al. 2016), two processes implicated in synaptic plasticity. Accordingly, lack of hevin prevents ocular dominance plasticity, which relies on synaptic rearrangement in the visual cortex (Singh et al. 2016). Although the role of astrocytic hevin in the adult brain is unclear, neuroanatomical studies show that hevin is ideally localized in these cells to modulate adult synaptic plasticity, as in the developing brain (Singh et al. 2016). Indeed, electron microscopy and confocal imaging have localized hevin in perisynaptic astrocytic processes of adult rodent brain (Jones et al. 2011; Kucukdereli et al. 2011; Lively and Brown 2008a; Risher et al. 2014; Singh et al. 2016; Weaver et al. 2010). Perisynaptic astrocytic processes are tightly connected with the majority of synapses (Ventura and Harris 1999), where they regulate glutamatergic neurotransmission (Anderson and Swanson 2000), spine maturation (Nishida and Okabe 2007), and ultimately control synaptic plasticity (Panatier et al. 2006). More importantly, calcium signals in astrocytic processes closely follow nearby neuronal activity evoked by sensory stimulation in awake mice (Shigetomi et al. 2013; Stobart et al. 2018). Because hevin possess several calcium-binding sites (Girard and Springer 1996; Hambrock et al. 2003), it could be engaged in the response to calcium signals in astrocytic processes, hence affecting synaptic plasticity in response to modifications of neuronal activity in the adult brain. In support of a role of

Table 4 Identity of hevin-expressing cells determined by double FISH in the mouse brain

Brain region	Astrocytes	GABAergic neurons					Glutamatergic neurons		Cholinergic neurons
	GLAST	PV	Sst	Calb	Cck	NPy	VGLUT1	VGLUT2	ChAT
Olfactory bulb									
Anterior olfactory nucleus	+	+	−	−	+	−	−		
Glomerular layer	+		−	−	−				
Mitral cell layer	+		−	−	+		+		
Periglomerular area	+		−	−	−		+		
Cortex									
Layer I	+								
Layer II-III	+	+	−	−	−	±	±		
Layer IV	+	+	−	−	−	±	±		
Layer V	+	+	−	−	−	±	±		
Layer VI	+	+	−	−	−	±	±		
Hippocampus									
Granular layer of dentate gyrus	+	+		−		+	+		
Molecular layer of dentate gyrus	+			−		±			
Polymorphic layer/Hilus	+	+	−	−	−	±	±		
CA3 Pyramidal cell layer	+	+		±	−	+	±		
CA3 Stratum oriens	+	+	−	±	−	+			
CA3 Stratum radiatum	+		−	−	−	+			
CA1 Pyramidal cell layer	+	+		±	−	−	−		
CA1 Stratum oriens	+	+	−	±	−	+			
CA1 Stratum radiatum	+	+	−	−	−	−			
CA2 Pyramidal cell layer	+	+					±		
Presubiculum	+	+	−	±		−	+		
Subiculum	+	+	−	±		−	+		
Indusium griseum	+	+					+		
Septohippocampal nucleus	−	+		−					
Septum									
Lateral septum	±		±	−		−			
Medial septum	+	+	−	−				±	
Basal nucleus	+			−					−
Basal ganglia									
Caudate putamen	+	+	−	−	−	−			−
Lateral globus pallidus	+	+							
Medial globus pallidus	+	+	+					+	
Amygdala									
Basolateral amygdala	+	+	−	−	−	±	−	±	
Central amygdala	+	+	−						
Medial amygdaloid nucleus	+	+	−	±	−	±	+	−	
Thalamus–hypothalamus									
Anterodorsal thalamic nucleus		+		−	−		±	+	
Anteroventral thalamic nucleus	+				−			+	
Hypothalamus	+	+	−	−				−	
Interanteromedial thalamic nucleus	+			−	−			−	
Lateral habenula	+			−				±	
Lateral mammillary nucleus	+							+	
Lateral posterior thalamic nucleus	+							+	
Laterodorsal thalamic nucleus	+			−	+		+	+	
Medial habenula	+			−					

Table 4 (continued)

Brain region	Astrocytes	GABAergic neurons					Glutamatergic neurons		Cholinergic neurons
	GLAST	PV	Sst	Calb	Cck	NPy	VGLUT1	VGLUT2	ChAT
Mediodorsal thalamic nucleus	+			−	−			−	
Paraventricular thalamic nucleus, anterior part	+							−	
Posterior thalamic nucleus	+			+					
Subthalamic nucleus								+	
Reticular thalamic nucleus	+	+	+			+			
Reuniens thalamic nucleus	+			−				−	
Ventral posteromedial thalamic nucleus	+	+		−	−		+	+	
Midbrain									
Anterior pretectal nucleus		+		±				±	
Dorsal lateral geniculate nucleus	+							+	
Intermediate nucleus of the lateral lemniscus		+						+	
Interpeduncular nucleus	+	+	−	−				±	
Laterotegmental nucleus	+								−
Nucleus of Darkschewitsch		+							
Oculomotor nucleus (III)	+	+	−						+
Pedunculopontine tegmental nucleus	+								−
Parabigeminal nucleus		+						+	
Prerubral field	+			−					
Red nucleus	+	+						+	
Substantia nigra pars compacta	+					−			
Substantia nigra pars reticulata	+	+							
Inferior colliculus	+	+		±		±			
Superior colliculus	+			−				±	
Zona incerta	+	+							
Cerebellum									
Bergmann glial cells	+								
Deep cerebellar nuclei		+						+	
Molecular layer	+	−						−	
Purkinje cell layer		−							
Pons									
Abducens nucleus (VI)	+	+							+
Ambiguus	+								−
Cochlear nucleus (VIII)	+	+		−				+	
Dorsal motor nucleus of vagus (X)	+								−
Facial nucleus (VII)	+								+
Hypoglossal nucleus (XII)	+								+
Lateral parabrachial nucleus	+								
Mesencephalic trigeminal nucleus	+	+		+			+	+	
Motor trigeminal nucleus (V)	+	±						±	+
Parabrachial nucleus	+	+	+	−			+	+	
Pontine reticular nucleus, oral part	+	+	±	±				+	
Principal sensory trigeminal nucleus	+	+		+			+	+	
Reticulotegmental nucleus of the pons	+	+	+	+			+	+	
Vestibular nucleus	+	+		+				+	

For each marker, (+) indicates that all cells express hevin mRNA, (±) indicates that only some cells express hevin mRNA, while some cells do not, and (−) indicates a lack of co-localization with hevin mRNA. Cells are left blank in the absence of the cellular marker. Monoaminergic nuclei are not indicated

Calb calbindin, *Cck* cholecystokinin, *GLAST* glutamate/aspartate transporter, *NPy* neuropeptide Y, *PV* parvalbumin, *Sst* somatostatin, *VGLUT* vesicular glutamate transporter

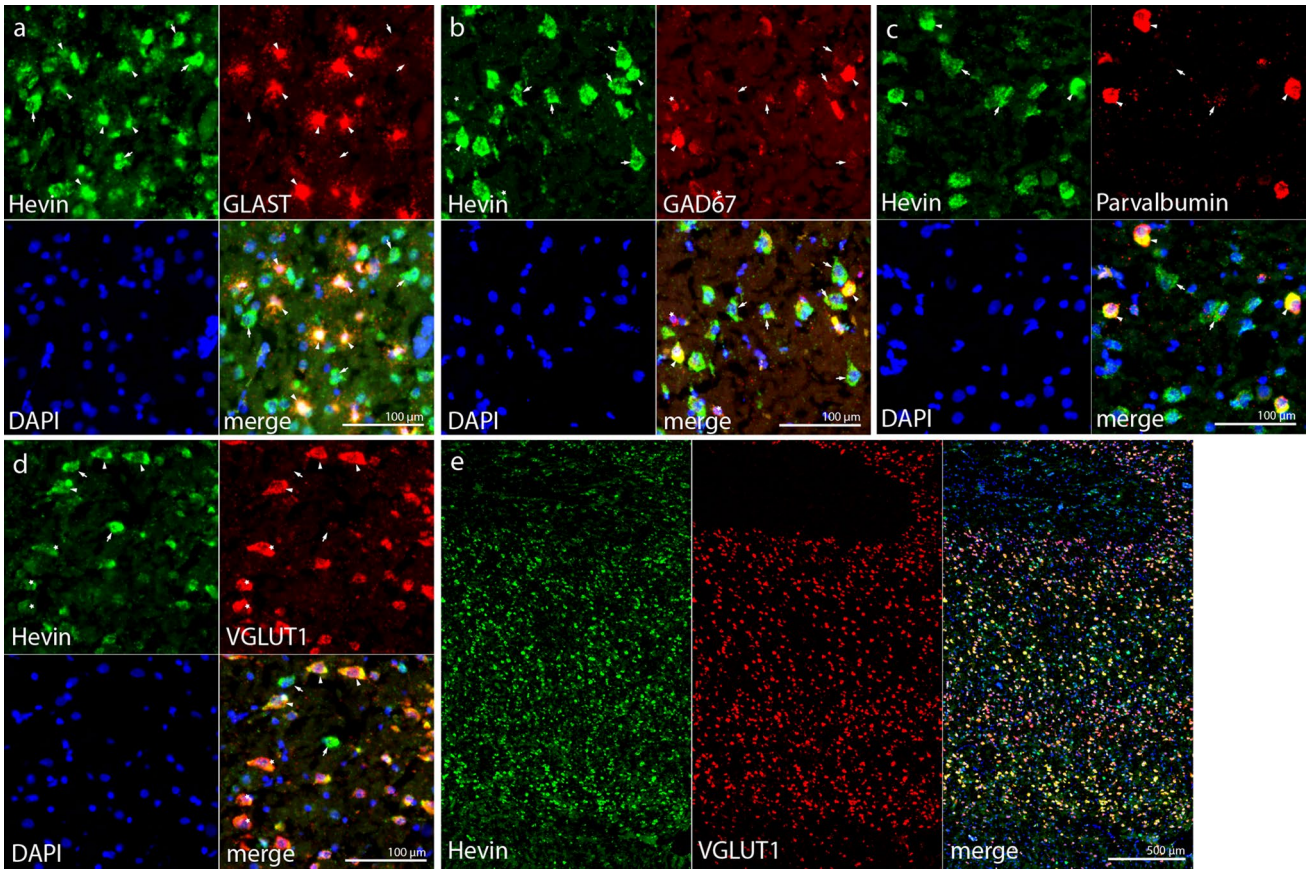

Fig. 11 Characterization of hevin mRNA-expressing cells in human prefrontal cortex. Hybridization signal for hevin mRNA (green) and GLAST (**a**), GAD67 (**b**), parvalbumin (**c**), and VGLUT1 (**d, e**) mRNA (red) is observed. In the cortex, representative photomicrographs obtained from the same human subject show co-localization (arrowhead) between hevin and GLAST, hevin and GAD67, hevin and parvalbumin, and hevin and VGLUT1. Hevin is expressed in most GLAST- and parvalbumin-positive cells (arrowhead), and partially in GAD67- and VGLUT1-positive cells (arrowhead and star). As expected, a substantial number of GLAST-, GAD67-, parvalbumin-, and VLGUT1-negative cells express hevin mRNA (arrow in **a**–**d**). At low magnification, hevin is observed with highest density in layers II/III and V/VI (**e**). This cellular profile of hevin mRNA expression was conserved in all the human cortical samples analyzed. DAPI signal is also presented (blue staining in the nucleus)

hevin in adult synaptic plasticity, hevin's binding partner neuroligin has been implicated in activity-dependent plasticity (Chubykin et al. 2007). Furthermore, the activity of hevin is controlled by extracellular proteases (Weaver et al. 2011, 2010), which are released upon neuronal activity and have been implicated in hippocampal long-term potentiation (Huntley 2012).

At first sight, it seems difficult to find a common denominator among the variety of neuron types expressing hevin. Interestingly, hevin is consistently absent from all monoaminergic neurons and forebrain cholinergic neurons. These neurons have a functionally different organization in the brain compared to glutamatergic and GABAergic neurons. Aminergic and cholinergic cell bodies are restricted to a small number of nuclei in the hindbrain, midbrain, hypothalamus and basal forebrain but their axons project widely throughout the forebrain. This organization allows these neurotransmitters to modulate the activity of diverse circuits. It thus appears that the expression of hevin in neurons is restricted to populations mediating fast excitatory and inhibitory synaptic transmission ensured by glutamatergic and GABAergic neurons, respectively. As proposed for astrocytes, intracellular calcium signals induced by neuronal activity could regulate hevin and in turn strengthen synaptic plasticity in glutamatergic and GABAergic neurons. In addition, hevin expression in almost all parvalbumin neurons, independently of their morphological differences, extent of axonal projection, differences in connectivity, presence of perineuronal nets and electrophysiological properties (Alberi et al. 2013; Mendez and Bacci 2011; Rossier et al. 2015), is in favor for a role in the specific properties of parvalbumin-expressing cells. Excitatory synapses onto parvalbumin neurons are modulated by the post-synaptic cell adhesion molecule

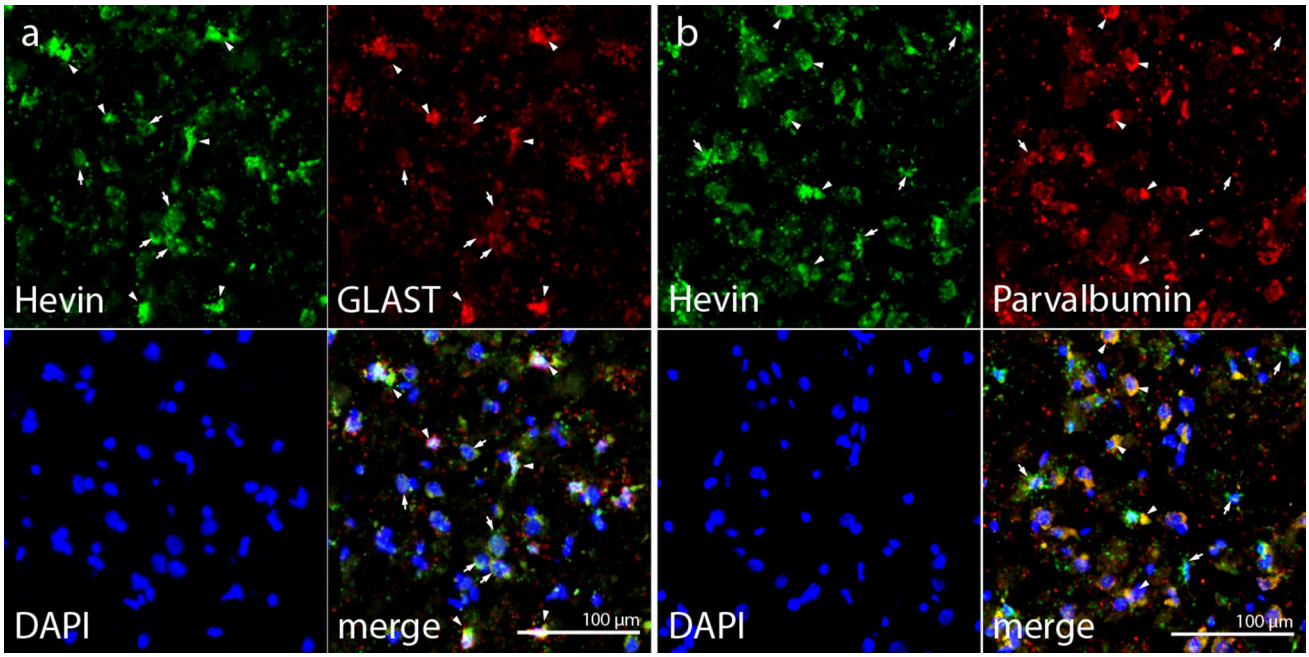

Fig. 12 Characterization of hevin mRNA-expressing cells in human caudate nucleus. Hybridization signal for hevin mRNA (green) and GLAST (**a**) and parvalbumin (**b**) mRNA (red) is observed. Representative photomicrographs obtained from two human subjects show co-localization (arrowhead) between hevin and GLAST (**a**), and hevin and parvalbumin (**b**). Hevin is expressed in most GLAST- and parvalbumin-positive cells (arrowhead). As expected, a number of GLAST- and parvalbumin-negative cells express hevin mRNA (arrow in **a, b**). This cellular profile of hevin mRNA expression was conserved in eight human caudate samples. DAPI signal is also presented (blue staining in the nucleus)

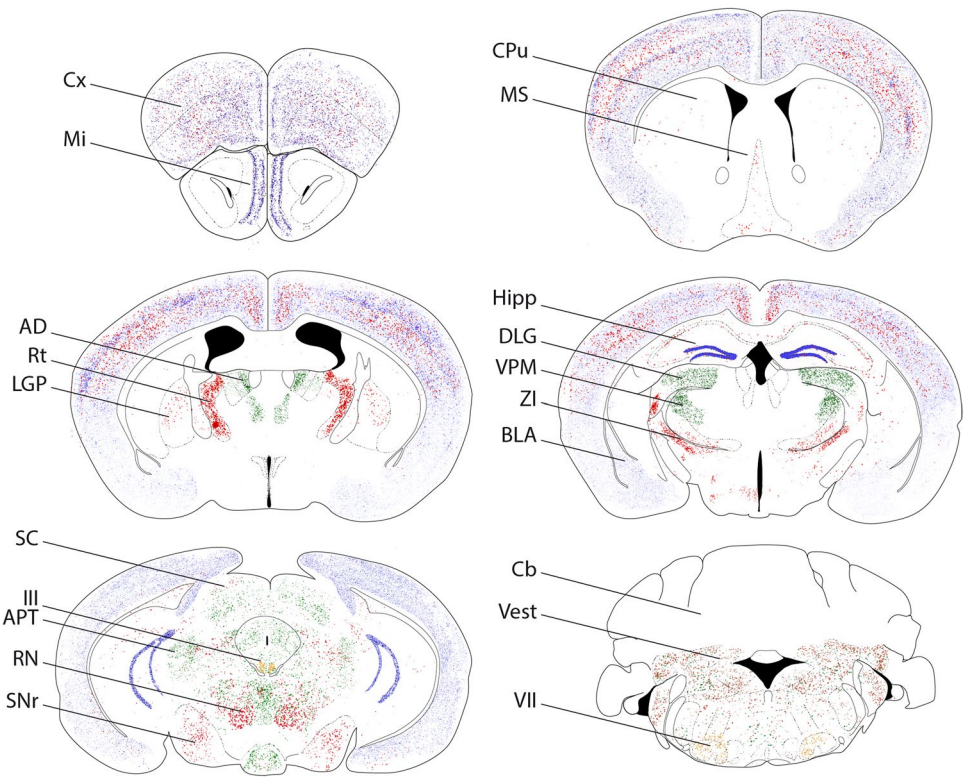

Fig. 13 Summary diagrams showing the regional distribution of hevin mRNA in glutamatergic (VGLUT1—blue, VGLUT2—green), parvalbumin (red), and cholinergic neurons (yellow) throughout the brain. Presence of hevin mRNA in astrocytes, which are expressed throughout the brain, is not indicated. See list of abbreviations

neuroligin 3 (Polepalli et al. 2017), which is a binding partner of hevin (Singh et al. 2016). Deletion of neuroligin 3 in parvalbumin interneurons of the hippocampus alters network activity by reducing gamma oscillations and sharp wave ripples, which specifically impairs contextual fear extinction (Polepalli et al. 2017). Thus, hevin could regulate network activity by modulating excitatory inputs into parvalbumin interneurons. Further studies will be necessary to determine the functional significance of hevin in parvalbumin neurons and other specific neuronal populations, using conditional cell-specific targeting of hevin expression.

Dysregulation of hevin protein levels has been associated with neurodegenerative and psychiatric diseases: hevin is among the most upregulated proteins detected in the cerebrospinal fluid of patients with Alzheimer's, Parkinson's disease, and multiple sclerosis (Hammack et al. 2004; Yin et al. 2009). Conversely, hevin protein levels are downregulated in postmortem prefrontal cortex samples of depressed patients (Zhurov et al. 2012). Hevin could contribute to the pathophysiology of these disorders by altering synaptic strength and morphology (Bernardinelli et al. 2014; Braak and Del Tredici 2008). Stress-induced depressive-like behaviors rely on changes in glutamate signaling, spine morphology and synaptic plasticity (Christoffel et al. 2011, 2015; Vialou et al. 2010). In agreement with a role of hevin in these processes, we previously found that hevin is induced in resilience to stress and is sufficient to induce an antidepressant response in adult mice (Vialou et al. 2010). This supports our hypothesis of a major role for hevin in higher cognitive functions in the adult.

Conclusions

Our neuroanatomical study in mouse and human brain distinguishes hevin from other matricellular proteins, and reveals a specific pattern of expression of hevin in subsets of neuronal populations throughout the adult brain. The cellular distribution of hevin is similar between human and mouse brain, suggesting an evolutionary conserved role for hevin in mammal adult CNS function. The function of hevin might depend on the specific cell type in which it is present. Hevin could contribute to adult synaptic plasticity mediated by astrocytes whereas its expression in parvalbumin neurons points to a fundamentally novel role in the regulation of network activity. This characterization of hevin expression profile will help dissect novel functions for this unique matricellular protein in the adult brain.

Acknowledgements This work was supported by funds from the Institut National de la Santé et de la Recherche Médicale (INSERM), Centre National de la Recherche Scientifique (CNRS), and Sorbonne Université, and by grants from the Brain & Behavior Research Foundation (NARSAD Young Investigator Award to VV, #17566), FP7 Marie Curie Actions Career Integration Grant (FP7-PEOPLE-2013-CIG #618807 to VV), Promouvoir l'Excellence de la Recherche à Sorbonne Université (PER-SU 2014 to VV), Agence Nationale de la Recherche (ANR JCJC 2015 Hevinsynapse to VV), the Basque Government (IT616/13 to JJM), Fondation pour la Recherche Médicale (DEQ20160334919 to EV), Fundación Vital (2018 to AME) and the European Foundation for Alcohol Research (EA 18 19 to LFC). The authors thank Etienne Audinat for the PV-Cre mice and Glenn Dallerac for the GFAP-CreER^{T2}. EP was a recipient of Marie Curie Intra-European Fellowship (IEF327648). LC has benefited from support by the Labex EpiGenMed (Investissements d'avenir #ANR-10-LABX-12-01). We thank Catalina Betancur for helpful discussions and comments on the manuscript; the staff members of the Basque Institute of Legal Medicine for processing the postmortem human brain samples; Stéphane Fouquet, David Godefroy, and Marie-Laure Niepon of the Imaging Facility at Institut de la Vision; Annick Prigeant of the Histology Facility at Institut du Cerveau et de la Moelle; and Chooyoung Baek and Audrey Pondaven for their help with the FISH experiments.

Compliance with ethical standards

Conflict of interest The authors declare that they have no conflict of interests.

Ethical approval All procedures performed in studies involving human participants were in accordance with the ethical standards of the institutional and/or national research committee and with the 1964 Helsinki declaration and its later amendments or comparable ethical standards. In addition, all applicable international, national, and/or institutional guidelines for the care and use of animals were followed.

Informed consent No consent is required for using leftover body material for scientific purposes from medico-legal autopsies.

References

Alberi L, Lintas A, Kretz R, Schwaller B, Villa AE (2013) The calcium-binding protein parvalbumin modulates the firing 1 properties of the reticular thalamic nucleus bursting neurons. J Neurophysiol 109:2827–2841. https://doi.org/10.1152/jn.00375.2012

Anderson CM, Swanson RA (2000) Astrocyte glutamate transport: review of properties, regulation, and physiological functions. Glia 32:1–14. https://doi.org/10.1002/1098-1136(200010)32:1%3C1::AID-GLIA10%3E3.0.CO;2-W

Apazoglou K, Farley S, Gorgievski V et al (2018) Antidepressive effects of targeting ELK-1 signal transduction. Nat Med 24:591–597. https://doi.org/10.1038/s41591-018-0011-0

Armstrong DM, Saper CB, Levey AI, Wainer BH, Terry RD (1983) Distribution of cholinergic neurons in rat brain: demonstrated by the immunocytochemical localization of choline acetyltransferase. J Comp Neurol 216:53–68. https://doi.org/10.1002/cne.902160106

Bernardinelli Y, Nikonenko I, Muller D (2014) Structural plasticity: mechanisms and contribution to developmental psychiatric disorders. Front Neuroanat 8:123. https://doi.org/10.3389/fnana.2014.00123

Blakely PK, Hussain S, Carlin LE, Irani DN (2015) Astrocyte matricellular proteins that control excitatory synaptogenesis are regulated by inflammatory cytokines and correlate with paralysis severity

during experimental autoimmune encephalomyelitis. Front Neurosci 9:344. https://doi.org/10.3389/fnins.2015.00344
Bornstein P (1995) Diversity of function is inherent in matricellular proteins: an appraisal of thrombospondin 1. J Cell Biol 130:503–506. https://doi.org/10.1083/jcb.130.3.503
Braak H, Del Tredici K (2008) Cortico-basal ganglia-cortical circuitry in Parkinson's disease reconsidered. Exp Neurol 212:226–229. https://doi.org/10.1016/j.expneurol.2008.04.001
Brekken RA, Sage EH (2000) SPARC, a matricellular protein: at the crossroads of cell-matrix. Matrix Biol 19:569–580
Cahoy JD, Emery B, Kaushal A et al (2008) A transcriptome database for astrocytes, neurons, and oligodendrocytes: a new resource for understanding brain development and function. J Neurosci 28:264–278. https://doi.org/10.1523/JNEUROSCI.4178-07.2008
Celio MR (1990) Calbindin D-28 k and parvalbumin in the rat nervous system. Neuroscience 35:375–475. https://doi.org/10.1016/0306-4522(90)90091-H
Chazalon M, Dumas S, Bernard JF et al (2018) The GABAergic Gudden's dorsal tegmental nucleus: a new relay for serotonergic regulation of sleep-wake behavior in the mouse. Neuropharmacology 138:315–330. https://doi.org/10.1016/j.neuropharm.2018.06.014
Christoffel DJ, Golden SA, Dumitriu D et al (2011) IkappaB kinase regulates social defeat stress-induced synaptic and behavioral plasticity. J Neurosci 31:314–321. https://doi.org/10.1523/JNEUROSCI.4763-10.2011
Christoffel DJ, Golden SA, Walsh JJ et al (2015) Excitatory transmission at thalamo-striatal synapses mediates susceptibility to social stress. Nat Neurosci 18:962–964. https://doi.org/10.1038/nn.4034
Chronwall BM, DiMaggio DA, Massari VJ, Pickel VM, Ruggiero DA, O'Donohue TL (1985) The anatomy of neuropeptide-Y-containing neurons in rat brain. Neuroscience 15:1159–1181. https://doi.org/10.1016/0306-4522(85)90260-X
Chubykin AA, Atasoy D, Etherton MR, Brose N, Kavalali ET, Gibson JR, Sudhof TC (2007) Activity-dependent validation of excitatory versus inhibitory synapses by neuroligin-1 versus neuroligin-2. Neuron 54:919–931. https://doi.org/10.1016/j.neuron.2007.05.029
Clemente-Perez A, Makinson SR, Higashikubo B et al (2017) Distinct thalamic reticular cell types differentially modulate normal and pathological cortical rhythms. Cell Rep 19:2130–2142. https://doi.org/10.1016/j.celrep.2017.05.044
Cui Q, Pitt JE, Pamukcu A et al (2016) Blunted mGluR activation disinhibits striatopallidal transmission in parkinsonian mice. Cell Rep 17:2431–2444. https://doi.org/10.1016/j.celrep.2016.10.087
Emsley JG, Macklis JD (2006) Astroglial heterogeneity closely reflects the neuronal-defined anatomy of the adult murine CNS. Neuron Glia Biol 2:175–186. https://doi.org/10.1017/S1740925X06000202
Erdozain AM, De Gois S, Bernard V et al (2018) Structural and functional characterization of the interaction of snapin with the dopamine transporter: differential modulation of psychostimulant actions. Neuropsychopharmacology 43:1041–1051. https://doi.org/10.1038/npp.2017.217
Eroglu C (2009) The role of astrocyte-secreted matricellular proteins in central nervous system development and function. J Cell Commun Signal 3:167–176. https://doi.org/10.1007/s12079-009-0078-y
Girard JP, Springer TA (1995) Cloning from purified high endothelial venule cells of hevin, a close relative of the antiadhesive extracellular matrix protein SPARC. Immunity 2:113–123. https://doi.org/10.1016/1074-7613(95)90083-7
Girard JP, Springer TA (1996) Modulation of endothelial cell adhesion by hevin, an acidic protein associated with high endothelial venules. J Biol Chem 271:4511–4517. https://doi.org/10.1074/jbc.271.8.4511
Gongidi V, Ring C, Moody M, Brekken R, Sage EH, Rakic P, Anton ES (2004) SPARC-like 1 regulates the terminal phase of radial glia-guided migration in the cerebral cortex. Neuron 41:57–69
Hambrock HO, Nitsche DP, Hansen U, Bruckner P, Paulsson M, Maurer P, Hartmann U (2003) SC1/hevin. An extracellular calcium-modulated protein that binds collagen I. J Biol Chem 278:11351–11358. https://doi.org/10.1074/jbc.M212291200
Hammack BN, Fung KY, Hunsucker SW, Duncan MW, Burgoon MP, Owens GP, Gilden DH (2004) Proteomic analysis of multiple sclerosis cerebrospinal fluid. Mult Scler 10:245–260. https://doi.org/10.1191/1352458504ms1023oa
Hashimoto N, Sato T, Yajima T et al (2016) SPARCL1-containing neurons in the human brainstem and sensory ganglion. Somatosens Mot Res 33:112–117. https://doi.org/10.1080/08990220.2016.1197115
Herculano-Houzel S (2014) The glia/neuron ratio: how it varies uniformly across brain structures and species and what that means for brain physiology and evolution. Glia 62:1377–1391. https://doi.org/10.1002/glia.22683
Herzog E, Bellenchi GC, Gras C et al (2001) The existence of a second vesicular glutamate transporter specifies subpopulations of glutamatergic neurons. J Neurosci 21:RC181
Huntley GW (2012) Synaptic circuit remodelling by matrix metalloproteinases in health and disease. Nat Rev Neurosci 13:743–757. https://doi.org/10.1038/nrn3320
Ingolia NT, Ghaemmaghami S, Newman JR, Weissman JS (2009) Genome-wide analysis in vivo of translation with nucleotide resolution using ribosome profiling. Science 324:218–223. https://doi.org/10.1126/science.1168978
Johansson O, Hokfelt T, Elde RP (1984) Immunohistochemical distribution of somatostatin-like immunoreactivity in the central nervous system of the adult rat. Neuroscience 13:265–339. https://doi.org/10.1016/0891-0618(91)90001-S
Johnston IG, Paladino T, Gurd JW, Brown IR (1990) Molecular cloning of SC1: a putative brain extracellular matrix glycoprotein showing partial similarity to osteonectin/BM40/SPARC. Neuron 4:165–176
Jones EV, Bernardinelli Y, Tse YC, Chierzi S, Wong TP, Murai KK (2011) Astrocytes control glutamate receptor levels at developing synapses through SPARC-beta-integrin interactions. J Neurosci 31:4154–4165. https://doi.org/10.1523/JNEUROSCI.4757-10.2011
Kucukdereli H, Allen NJ, Lee AT et al (2011) Control of excitatory CNS synaptogenesis by astrocyte-secreted proteins Hevin and SPARC. Proc Natl Acad Sci USA 108:E440–E449. https://doi.org/10.1073/pnas.1104977108
Lively S, Brown IR (2008a) Extracellular matrix protein SC1/hevin in the hippocampus following pilocarpine-induced status epilepticus. J Neurochem 107:1335–1346. https://doi.org/10.1111/j.1471-4159.2008.05696.x
Lively S, Brown IR (2008b) The extracellular matrix protein SC1/hevin localizes to excitatory synapses following status epilepticus in the rat lithium-pilocarpine seizure model. J Neurosci Res 86:2895–2905. https://doi.org/10.1002/jnr.21735
Lively S, Brown IR (2008c) Localization of the extracellular matrix protein SC1 coincides with synaptogenesis during rat postnatal development. Neurochem Res 33:1692–1700. https://doi.org/10.1007/s11064-008-9606-z
Lively S, Moxon-Emre I, Schlichter LC (2011) SC1/hevin and reactive gliosis after transient ischemic stroke in young and aged rats. J Neuropathol Exp Neurol 70:913–929. https://doi.org/10.1097/NEN.0b013e318231151e
Lloyd-Burton S, Roskams AJ (2012) SPARC-like 1 (SC1) is a diversely expressed and developmentally regulated matricellular protein that does not compensate for the absence of SPARC in the CNS. J Comp Neurol 520:2575–2590. https://doi.org/10.1002/cne.23029
Markiewicz I, Lukomska B (2006) The role of astrocytes in the physiology and pathology of the central nervous system. Acta Neurobiol Exp (Wars) 66:343–358

McKinnon PJ, McLaughlin SK, Kapsetaki M, Margolskee RF (2000) Extracellular matrix-associated protein Sc1 is not essential for mouse development. Mol Cell Biol 20:656–660. https://doi.org/10.1128/MCB.20.2.656-660.2000

Mendez P, Bacci A (2011) Assortment of GABAergic plasticity in the cortical interneuron melting pot. Neural Plast 2011:976856. https://doi.org/10.1155/2011/976856

Mendis DB, Malaval L, Brown IR (1995) SPARC, an extracellular matrix glycoprotein containing the follistatin module, is expressed by astrocytes in synaptic enriched regions of the adult brain. Brain Res 676:69–79

Mendis DB, Shahin S, Gurd JW, Brown IR (1996) SC1, a SPARC-related glycoprotein, exhibits features of an ECM component in the developing and adult brain. Brain Res 713:53–63

Mendis DB, Ivy GO, Brown IR (2000) Induction of SC1 mRNA encoding a brain extracellular matrix glycoprotein related to SPARC following lesioning of the adult rat forebrain. Neurochem Res 25:1637–1644

Morel L, Chiang MSR, Higashimori H et al (2017) Molecular and Functional Properties of Regional Astrocytes in the Adult Brain. J Neurosci 37:8706–8717. https://doi.org/10.1523/JNEUROSCI.3956-16.2017

Mothe AJ, Brown IR (2002) Effect of hyperthermia on the transport of mRNA encoding the extracellular matrix glycoprotein SC1 into Bergmann glial cell processes. Brain Res 931:146–158. https://doi.org/10.1016/S0006-8993(02)02270-9

Murphy-Ullrich JE, Sage EH (2014) Revisiting the matricellular concept. Matrix Biol 37:1–14. https://doi.org/10.1016/j.matbio.2014.07.005

Nedergaard M, Ransom B, Goldman SA (2003) New roles for astrocytes: redefining the functional architecture of the brain. Trends Neurosci 26:523–530. https://doi.org/10.1016/j.tins.2003.08.008

Nishida H, Okabe S (2007) Direct astrocytic contacts regulate local maturation of dendritic spines. J Neurosci 27:331–340. https://doi.org/10.1523/JNEUROSCI.4466-06.2007

Panatier A, Theodosis DT, Mothet JP, Touquet B, Pollegioni L, Poulain DA, Oliet SH (2006) Glia-derived D-serine controls NMDA receptor activity and synaptic memory. Cell 125:775–784. https://doi.org/10.1016/j.cell.2006.02.051

Paxinos G, Franklin KBG (2001) The mouse brain in stereotaxic coordinates, 2nd edn. Academic, San Diego

Polepalli JS, Wu H, Goswami D, Halpern CH, Sudhof TC, Malenka RC (2017) Modulation of excitation on parvalbumin interneurons by neuroligin-3 regulates the hippocampal network. Nat Neurosci 20:219–229. https://doi.org/10.1038/nn.4471

Risher WC, Patel S, Kim IH et al (2014) Astrocytes refine cortical connectivity at dendritic spines. Elife. https://doi.org/10.7554/eLife.04047

Rossier J, Bernard A, Cabungcal JH et al (2015) Cortical fast-spiking parvalbumin interneurons enwrapped in the perineuronal net express the metallopeptidases Adamts8, Adamts15 and Neprilysin. Mol Psychiatry 20:154–161. https://doi.org/10.1038/mp.2014.162

Sage EH, Bornstein P (1991) Extracellular proteins that modulate cell-matrix interactions—sparc, tenascin, and thrombospondin. J Biol Chem 266:14831–14834

Savasta M, Palacios JM, Mengod G (1988) Regional localization of the mRNA coding for the neuropeptide cholecystokinin in the rat brain studied by in situ hybridization. Neurosci Lett 93:132–138. https://doi.org/10.1016/0169-328X(90)90086-S

Schmitt A, Asan E, Puschel B, Kugler P (1997) Cellular and regional distribution of the glutamate transporter GLAST in the CNS of rats: nonradioactive in situ hybridization and comparative immunocytochemistry. J Neurosci 17:1–10

Schweizer N, Pupe S, Arvidsson E et al (2014) Limiting glutamate transmission in a Vglut2-expressing subpopulation of the subthalamic nucleus is sufficient to cause hyperlocomotion. Proc Natl Acad Sci USA 111:7837–7842. https://doi.org/10.1073/pnas.1323499111

Shigetomi E, Bushong EA, Haustein MD et al (2013) Imaging calcium microdomains within entire astrocyte territories and endfeet with GCaMPs expressed using adeno-associated viruses. J Gen Physiol 141:633–647. https://doi.org/10.1085/jgp.201210949

Singh SK, Stogsdill JA, Pulimood NS et al (2016) Astrocytes assemble thalamocortical synapses by bridging NRX1alpha and NL1 via Hevin. Cell 164:183–196. https://doi.org/10.1016/j.cell.2015.11.034

Soderling JA, Reed MJ, Corsa A, Sage EH (1997) Cloning and expression of murine SC1, a gene product homologous to SPARC. J Histochem Cytochem 45:823–835. https://doi.org/10.1177/002215549704500607

Stobart JL, Ferrari KD, Barrett MJP, Gluck C, Stobart MJ, Zuend M, Weber B (2018) Cortical circuit activity evokes rapid astrocyte calcium signals on a similar timescale to neurons. Neuron 98:726–735 e724. https://doi.org/10.1016/j.neuron.2018.03.050

Sullivan MM, Puolakkainen PA, Barker TH, Funk SE, Sage EH (2008) Altered tissue repair in hevin-null mice: inhibition of fibroblast migration by a matricellular SPARC homolog. Wound Repair Regen 16:310–319. https://doi.org/10.1111/j.1524-475X.2008.00370.x

Tepper JM, Tecuapetla F, Koos T, Ibanez-Sandoval O (2010) Heterogeneity and diversity of striatal GABAergic interneurons. Front Neuroanat 4:150. https://doi.org/10.3389/fnana.2010.00150

Ventura R, Harris KM (1999) Three-dimensional relationships between hippocampal synapses and astrocytes. J Neurosci 19:6897–6906. https://doi.org/10.1523/JNEUROSCI.19-16-06897.1999

Vialou V, Balasse L, Dumas S, Giros B, Gautron S (2007) Neurochemical characterization of pathways expressing plasma membrane monoamine transporter in the rat brain. Neuroscience 144:616–622. https://doi.org/10.1016/j.neuroscience.2006.09.058

Vialou V, Robison AJ, Laplant QC et al (2010) DeltaFosB in brain reward circuits mediates resilience to stress and antidepressant responses. Nat Neurosci 13:745–752. https://doi.org/10.1038/nn.2551

Viereckel T, Dumas S, Smith-Anttila CJ et al (2016) Midbrain gene screening identifies a new mesoaccumbal glutamatergic pathway and a marker for dopamine cells neuroprotected in Parkinson's disease. Sci Rep 6:35203. https://doi.org/10.1038/srep35203

Vincent AJ, Lau PW, Roskams AJ (2008) SPARC is expressed by macroglia and microglia in the developing and mature nervous system. Dev Dyn 237:1449–1462. https://doi.org/10.1002/dvdy.21495

Weaver MS, Workman G, Cardo-Vila M, Arap W, Pasqualini R, Sage EH (2010) Processing of the matricellular protein hevin in mouse brain is dependent on ADAMTS4. J Biol Chem 285:5868–5877. https://doi.org/10.1074/jbc.M109.070318

Weaver M, Workman G, Schultz CR, Lemke N, Rempel SA, Sage EH (2011) Proteolysis of the matricellular protein hevin by matrix metalloproteinase-3 produces a SPARC-like fragment (SLF) associated with neovasculature in a murine glioma model. J Cell Biochem. https://doi.org/10.1002/jcb.23235

Yin GN, Lee HW, Cho JY, Suk K (2009) Neuronal pentraxin receptor in cerebrospinal fluid as a potential biomarker for neurodegenerative diseases. Brain Res 1265:158–170. https://doi.org/10.1016/j.brainres.2009.01.058

Zeisel A, Munoz-Manchado AB, Codeluppi S et al (2015) Brain structure. Cell types in the mouse cortex and hippocampus revealed by single-cell RNA-sEq. Science 347:1138–1142. https://doi.org/10.1126/science.aaa1934

Zhurov V, Stead JD, Merali Z et al (2012) Molecular pathway reconstruction and analysis of disturbed gene expression in depressed individuals who died by suicide. PLoS One 7:e47581. https://doi.org/10.1371/journal.pone.0047581